Derivation of a Non-Local Model for Diffusion Asymptotics; Application to Radiative Transfer Problems

C. Besse[1,2]*and T. Goudon[1,2]

[1]*Project Team SIMPAF, INRIA Lille Nord Europe Research Centre Park Plazza, 40 avenue Halley, F-59650 Villeneuve d'Ascq, France*
[2] *Laboratoire Paul Painlevé, UMR 8524, CNRS–Université des Sciences et Technologies de Lille, Cité Scientifique, F-59655 Villeneuve d'Ascq Cedex, France*

Abstract. In this paper, we introduce a moment closure which is intended to provide a macroscopic approximation of the evolution of a particle distribution function, solution of a kinetic equation. This closure is of non local type in the sense that it involves convolution or pseudo-differential operators. We show it is consistent with the diffusion limit and we propose numerical approximations to treat the non local terms. We illustrate how this approach can be incorporated in complex models involving a coupling with hydrodynamic equations, by treating examples arising in radiative transfer. We pay a specific attention to the conservation of the total energy by the numerical scheme.

AMS subject classifications: 35Q99 35B25

Key words: Diffusion approximation. Nonlocal transport. Asymptotic preserving methods. Radiative hydrodynamics.

1 Introduction

We are interested in the derivation of "intermediate models", intended to capture the essential features of the solutions of the following kinetic equation

$$\varepsilon\partial_t f_\varepsilon + a(v)\cdot\nabla_x f_\varepsilon = \frac{1}{\varepsilon}\,Q(f_\varepsilon) \tag{1.1}$$

for small values of the parameter $\varepsilon>0$. This equation arises when describing the evolution of many "particles" described by their distribution function in phase space $f_\varepsilon(t,x,v)$: $t\geq 0$, $x\in\mathbb{R}^N$ stand for the time and space variables, respectively while the variable v — which lies in some measured space $(\mathcal{V},\mathrm{d}v)$, $\mathcal{V}\subset\mathbb{R}^M$ — represents some physical state of the

*Corresponding author. *Email addresses:* christophe.besse@math.univ-lille1.fr (C. Besse), thierry.goudon@inria.fr (T. Goudon)

particles. The word "particles" might refer to very different physical situations: they could be gas molecules, neutrons, electrons or ions, photons, stars or planets or even bacteria... In this paper, we shall be mainly concerned with the case where (1.1) models the evolution of radiation energy (but our approach applies to a general framework). The function $a:\mathcal{V}\to\mathbb{R}^N$ associates to a state v the velocity $a(v)$ and the left hand side in (1.1) describes the transport of the particles whereas Q is a "collision operator" intended to describe the interaction processes the particles are subject to. In most of the applications this operator acts only on the variable v. The most common framework is $a(v)=v\in\mathbb{R}^N$, $\mathcal{V}=\mathbb{R}^N$ or $\mathcal{V}=\mathbb{S}^{N-1}$ endowed with the Lebesgue measure, but more complicated models can be dealt with. The equation (1.1) is written in dimensionless form and the parameter ε is associated to the mean free path of the particles. As $\varepsilon\to 0$ the solution of (1.1) tends towards an equilibrium state which makes the collision operator vanish $f_\varepsilon\simeq f_{\rm eq}$, $Q(f_{\rm eq})=0$. Therefore, this fixes the dependence with respect to the variable v, and the dynamics reduces to a diffusion equation satisfied by some macroscopic quantities, which means some $v-$average of the unknown.

However for many applications, such a convergence statement is not sufficient; instead, one would be interested in a model for intermediate regimes, for small, but non zero ε's. For instance, the diffusion equation propagates information with infinite speed, while the speed of propagation of the original model is v/ε. There exists a huge literature on possible ways to derive a model "in-between" the fully microscopic description and the limit diffusion equation. The question is particularly relevant for numerical purposes since computing the solution of (1.1) for small ε's becomes rapidly non affordable. Very often these reduced models are constructed with a suitable closure of the equations satisfied by moments with respect to v of f_ε. We refer for instance to [32,33,36] for presentation and comparison of such closures. Among others the closure based on entropy minimization principle, which is referred to as the $M1$ model, received a lot of attention, see [20,21,26,34,35]; it is used for numerical simulations in radiative transfer [8–10]. The well-posedness and consistency with the diffusion asymptotics have been established rigorously in [15] and for numerical experiments we refer to [13]. For recent progress on moment closures, we refer also to [53].

This work is devoted to another class of reduced models which are of nonlocal or, more precisely, of pseudo-differential nature. These nonlocal models have been introduced for complex kinetic equations arising in plasma physics, and they are currently used in numerical simulations of fusion plasmas. The introduction of such models dates back to [42,43], and we refer to further discussions and improvements to [1,24,25,45,47, 50,51,57]. The objectives of the present contribution can be summarized as follows:

- We wish to make clear the derivation of the nonlocal model starting from a kinetic equation as simple as possible;

- Then, we analyze the main properties of the pseudo-differential equation, in particular the well-posedness and consistency to the diffusion approximation;

- And we discuss the possible approximations of the nonlocal term amenable to tractable numerical treatments.

Since in practice the kinetic equation is involved in a coupled system of PDEs, where each equation induce its own numerical constraints, see e. g. [45, 51, 57], we illustrate how the numerical treatment can be adapted to such a complex situation, by discussing a coupling with hydrodynamics motivated by radiative transfer applications. Indeed, the application to radiative transfer is well adapted to our purpose. The collision operator describes both scattering and energy exchanges between photons and the material and it usually has a quite simple expression. However, the kinetic equation for the radiative intensity is coupled to the evolution of the properties of the surrounding gas, described by the hydrodynamic system (Euler equations for instance). We discuss in details how the coupling can be handled, paying particular attention to the conservation of the total energy which prohibits a too naive splitting approach.
This work is organized as follows. In Section 2, we set up a few notations and we recall the derivation of the diffusion regime for a simple linear operator Q, say relaxation or Fokker-Planck operator. Then, we introduce the non local model. In Section 3 we discuss some mathematical properties of the model. Section 4 is concerned with further approximations, having in mind numerical purposes. Finally, we describe how the modeling adapts to more complex situations motivated by radiative transfer problems in Section 5.

2 Diffusion Regime and Non Local Model

Even if our approach can be adapted to treat general situations, we restrict the presentation for the sake of clarity to linear collision operators. We first introduce the main assumptions on which the diffusion asymptotics is based. Second, we recall the derivation of the limit equation. Finally, we modify the Hilbert expansion to derive the non local model.

2.1 Collision Operator and Equilibrium; Examples

We recall that $\mathcal{V}$ is a subset of $\mathbb{R}^M$ endowed with a measure $\mathrm{d}v$ and a is an application $\mathbb{R}^M \to \mathbb{R}^N$. In this paper, Q is a linear operator verifying the conservation property

$$\int_{\mathcal{V}} Q(f)\,\mathrm{d}v = 0.$$

It means that the collision processes do not modify the total number of particles and consequently the integration of (1.1) with respect to the variable v yields the conservation equation

$$\partial_t \int_{\mathcal{V}} f_\varepsilon \mathrm{d}v + \nabla_x \cdot \int_{\mathcal{V}} \frac{a(v)}{\varepsilon} f_\varepsilon \mathrm{d}v = 0$$

(conservation of mass or conservation of charge or conservation of energy... depending on the physical context). As ε goes to 0, we expect to obtain a closed (diffusion) equation for the macroscopic density of particles which relies on obtaining a relation between the flux $\lim_{\varepsilon\to 0}\int_{\mathcal{V}}\frac{a(v)}{\varepsilon}f_\varepsilon \mathrm{d}v$ and the macroscopic density $\lim_{\varepsilon\to 0}\int_{\mathcal{V}} f_\varepsilon \mathrm{d}v$. This asymptotics relies on several assumptions on Q and a that we list now. More assumptions will be introduced for the derivation of useful formulae when discussing the non local models. The relevance of these hypothesis will be illustrated through a couple of examples.

2.1.1 Requirements on the equilibrium and velocity function

As mentioned above, a crucial role is played by the elements of the kernel of Q; hence, we start with

Assumption 2.1. There exists $\mathcal{M}:\mathcal{V}\to\mathbb{R}$ verifying:

$$\mathcal{M}(v)>0,\qquad \mathcal{M}\in L^1\cap L^\infty(\mathcal{V}),\qquad \int_{\mathcal{V}}\mathcal{M}(v)\mathrm{d}v=1,\qquad Q(\mathcal{M})=0.$$

The collision processes have a relaxation effect which forces the solution of (1.1) to resembles an equilibrium. This is related to dissipation mechanisms that we rephrase here as a spectral gap property.

Assumption 2.2. We set $H=L^2(\mathcal{V},\frac{1}{\mathcal{M}(v)}\mathrm{d}v)$. The kernel of Q is one-dimensional and more precisely

$$\mathrm{Ker}(Q)=\mathrm{Span}(\mathcal{M})\subset H.$$

Furthermore, there exists a constant $\kappa>0$ such that

$$-\int_{\mathcal{V}}Q(f)\frac{f}{\mathcal{M}}\mathrm{d}v=-(Q(f),f)_H\geq\kappa\int_{\mathcal{V}}|f-\langle f\rangle\mathcal{M}|^2\,\frac{\mathrm{d}v}{\mathcal{M}(v)}=\kappa\|f-\langle f\rangle\mathcal{M}\|_H^2,$$

where $\langle f\rangle=\int_{\mathcal{V}}f\,\mathrm{d}v$.

Remark 2.1. The space $H=\{f:\mathcal{V}\to\mathbb{R},\ \int_{\mathcal{V}}f^2/\mathcal{M}\mathrm{d}v<\infty\}$ embeds to $L^1(\mathcal{V})$ as a consequence of the Cauchy-Schwarz inequality.

We also need the the following Fredholm alternative type property.

Assumption 2.3. Let $h\in H$. Then, the problem $Q(f)=h$ has a solution $f\in H$ iff $\langle h\rangle=0$. The solution is unique in $\{g\in H,\ \langle g\rangle=0\}$ and satisfies $\|f\|_H\leq\kappa^{-1}\|h\|_H$.

Next, the diffusion regime requires some conditions involving the velocity function $v\mapsto a(v)$.

Assumption 2.4. The following properties are fulfilled:

i) $(1+|a(v)|^3)\mathcal{M}(v)\in L^1(\mathcal{V})$,

ii) We have

$$\int_{\mathcal{V}} a(v)\ \mathcal{M}(v)\mathrm{d}v = 0,$$

iii) The matrix $D_0 = \int_{\mathcal{V}} a(v)\otimes a(v)\mathcal{M}(v)\mathrm{d}v$ is positive definite.

Assumption i) is only an integrability property which justifies the finiteness of high order moment of the equilibrium. The null flux assumption ii) is crucial, it makes the scaling in (1.1) relevant. As a matter of fact, it allows to define $\chi \in H$ solution of

$$Q(\chi) = -a(v)\mathcal{M}(v), \qquad \langle \chi \rangle = 0 \tag{2.1}$$

by using Assumption 2.3. The last assumption iii) leads to the positiveness of the coefficients of the limit equation (see (2.9) below).

Lemma 2.1. *Let Assumptions 2.1–2.4 be satisfied. Let us set*

$$\mathcal{D} = \int_{\mathcal{V}} a(v)\otimes\chi\mathrm{d}v.$$

There exists $\alpha > 0$ such that for any $\xi \in \mathbb{R}^N$, we have $\mathcal{D}\xi\cdot\xi \geq \alpha|\xi|^2$.

Proof. Definition (2.1) yields

$$\mathcal{D}\xi\cdot\xi = -\int_{\mathcal{V}} Q(\chi\cdot\xi)\ \chi\cdot\xi\frac{\mathrm{d}v}{\mathcal{M}(v)} \geq \kappa\int_{\mathcal{V}}|\chi\cdot\xi|^2\frac{\mathrm{d}v}{\mathcal{M}(v)} \geq 0.$$

Moreover, $\mathcal{D}\xi\cdot\xi = 0$ implies that $\chi(v)\cdot\xi = 0$ for a. e $v \in \mathcal{V}$, and accordingly, $Q(\chi\cdot\xi) = -a(v)\mathcal{M}(v)\cdot\xi = 0$. It follows that $D_0\xi\cdot\xi = \int_{\mathcal{V}}|a(v)\cdot\xi|^2\mathcal{M}(v)\mathrm{d}v = 0$. Assumption 2.4- iii) then tells us that this happens for $\xi = 0$ only. We conclude that $\xi \mapsto \mathcal{D}\xi\cdot\xi$ is a continuous and positive function on the sphere $\mathbb{S}^{N-1}$ and we can define $\alpha > 0$ as to be its minimum. ∎

Finally, our discussion on intermediate models will use further symmetry assumptions in order to derive tractable formulas.

Assumption 2.5. The following properties are fulfilled

i) If $v \in \mathcal{V}$, so does $-v$; and $v \mapsto a(v)$ is odd,

ii) $\mathcal{M}(v) = M(|v|)$ depends only on $|v|$,

iii) There exists $\lambda : \mathbb{R}^+ \to \mathbb{R}$ bounded such that

$$Q\big(a(v)\lambda(|v|)\ \mathcal{M}(v)\big) = -a(v)\ \mathcal{M}(v),$$

that is $\chi(v) = a(v)\lambda(|v|)\ \mathcal{M}(v)$.

2.1.2 Examples

Let us describe now a few relevant situations in which the set of assumptions described above is fulfilled. We can consider a linear integral operator that splits into a gain non local operator and a loss term as follows

$$Q(f)(v) = \int_{\mathcal{V}} b(v,v_\star) f(v_\star)\,\mathrm{d}v_\star - B(v) f(v) \tag{2.2}$$

where

$$\begin{aligned} &b : \mathcal{V}\times\mathcal{V} \to \mathbb{R} \qquad 0 < \underline{b} \le b(v,v_\star) \le \overline{b}, \\ &B : \mathcal{V} \to \mathbb{R} \qquad 0 < \underline{b} \le B(v) \le \overline{b} \end{aligned}$$

are given (smooth) functions. The conservation property is equivalent to

$$B(v) = \int_{\mathcal{V}} b(v_\star,v)\,\mathrm{d}v_\star.$$

The verification of the dissipation property and the Fredholm alternative in Assumptions 2.2 and 2.3 can be found in [18] where a much more general functional framework is considered, with a complete analysis of the diffusion asymptotics.

In most of the applications, we simply have

$$\mathcal{V} \subset \mathbb{R}^N, \qquad a(v) = v$$

with one among the following definitions:

$$N = 1 \text{ and } \mathcal{V} = (-1,+1) \text{ endowed with the (normalized) Lebesgue measure,} \tag{2.3}$$

$$N > 1, \mathcal{V} = \mathbb{S}^{N-1} \text{ endowed with the (normalized) Lebesgue measure,} \tag{2.4}$$

$$\mathcal{V} \subset \mathbb{R}^N \text{ (possibly } \mathcal{V} = \mathbb{R}^N\text{) endowed with the Lebesgue measure,} \tag{2.5}$$

$$\mathcal{V} = \mathbb{R} \text{ endowed with the discrete measure } \mathrm{d}v = \tfrac{1}{2}(\delta_{v=-1} + \delta_{v=+1}), \tag{2.6}$$

$$\mathcal{V} = \mathbb{R}^N \text{ endowed with the discrete measure } \mathrm{d}v = \textstyle\sum_{i=1}^{P} \omega_i \delta_{v=v^i} \tag{2.7}$$

for a set $\{v^1,\dots,v^P\}$ of given vectors in $\mathbb{R}^M$, and positive weights $\omega_i > 0$.

The simplest example is given by the relaxation operator

$$Q(f) = \sigma\big(\langle f\rangle \mathcal{M}(v) - f\big), \tag{2.8}$$

where $\sigma > 0$ (it means that in (2.2) we set $b(v,v_\star) = \sigma\mathcal{M}(v)$) and:

- For Examples (2.3), (2.4), (2.6) or (2.7), we set $\mathcal{M}(v) = 1$,
- For Example (2.5) with $\mathcal{V} = \mathbb{R}^N$, the equilibrium is the normalized Maxwellian $\mathcal{M}(v) = (2\pi)^{-N/2} e^{-v^2/2}$.

Note that for this specific operator we simply have $\chi(v) = \frac{v}{\sigma}\mathcal{M}(v)$.

Remark 2.2. For Example (2.7), the conservation property recasts as $\sum_{i=1}^{P}\omega_i = 1$; then Assumption 2.4-ii) implies that the $a(v_i)$'s are linearly dependent whereas iii) means that $\{a(v^1),\dots,a(v^P)\}$ is generator in $\mathbb{R}^N$ (and in particular $P > N$), see [29].

Another example is given by a differential operator: with the Lebesgue measure on $\mathcal{V} = \mathbb{R}^N$, and $a(v) = v$, we can consider the linear Fokker-Planck operator

$$Q(f) = \sigma\nabla_v\cdot\big(vf + \nabla_v f\big) = \sigma\nabla_v\cdot\big(\mathcal{M}\nabla_v(f/\mathcal{M})\big), \qquad \mathcal{M}(v) = (2\pi)^{-N/2}e^{-v^2/2}.$$

Again, we remark that $\chi(v) = \frac{v}{\sigma}\mathcal{M}(v)$.

The properties in Assumption 2.5 remain quite general and they can be checked under simple symmetry assumptions on the coefficients, as shown in [19].

Lemma 2.2. *Suppose that $\mathcal{V} \subset \mathbb{R}^N$. Assume that for any isometry $R \in O(\mathbb{R}^N)$, we have*

$$a(Rv) = Ra(v)$$

and

$$Q(f\circ R) = Q(f)\circ R.$$

Then the properties in Assumption 2.5 hold.

Proof. The proof is due to [19] and we only sketch the arguments. First, we observe that $Q(\mathcal{M}\circ R) = Q(\mathcal{M})\circ R = 0$ so that $\mathcal{M}\circ R = \mathcal{M}$ and $\mathcal{M}$ is radially symmetric. Second, we have $Q(\chi)(Rv) = -a(Rv)\mathcal{M}(Rv) = Ra(v)M(|v|)$ which implies $\chi\circ R = R\chi$. Then, Lemma 3 in [19] proves that $\chi(v) = -a(v)\lambda(|v|)M(|v|)$. ∎

Equation (1.1) with $a(v) = v$ and Q given by (2.2) is a standard model in neutron transport, $\mathcal{V}$ being some bounded domain in $\mathbb{R}^N$ as in (2.5), see [17] (Vol. 3, Chap. XXI, pp. 1075 and ff.) or [48]. With $\mathcal{V} = \mathbb{S}^{N-1}$, see (2.4), it appears as a simplified model in radiative transfer theory. Assumption 2.5 is therefore fulfilled when the kernel $b(v,v_\star)$ depends only on $v\cdot v_\star$ (isotropic medium). Then $B(v) = \int_{\mathbb{S}^{N-1}} b(v\cdot v_\star)\,\mathrm{d}v_\star = \beta$ is constant and $\mathcal{M}(v) = 1$. We define the mean scattering cosine

$$\bar{\mu}_0\, v = \int_{\mathbb{S}^{N-1}} v_\star\, \sigma_0(v\cdot v_\star)\,\mathrm{d}v_\star,$$

where $\bar{\mu}_0$ is a constant independent of v. We always have $|\bar{\mu}_0| < \beta$ and the auxiliary function $\chi(v)$ is given by $(\beta - \bar{\mu}_0)^{-1}\, v$.

Lemma 2.2 allows to describe further examples. We suppose that the velocity function derives from an energy function

$$a(v) = \nabla\mathscr{E}(v), \qquad v \in \mathbb{R}^N$$

with $\mathscr{E}:\mathbb{R}^N\to\mathbb{R}$. The energy is usually a radially symmetric function. The case $a(v)=v$ simply corresponds to $\mathscr{E}(v)=v^2/2$. Relativistic models lead to

$$\mathscr{E}(v)=\sqrt{1+v^2}-1,\qquad a(v)=\frac{v}{\sqrt{1+v^2}}.$$

A similar formula appears in semiconductor theory when using correction to the parabolic band approximation based on the Kane dispersion relation, $\mathscr{E}(1+\mathscr{E})=v^2/2$, see [54]. Another possible correction is

$$\mathscr{E}(v)=\frac{v^2}{1+\sqrt{1+2\alpha v^2}}$$

with $\alpha>0$, the so-called non parabolic parameter, see [12]. Within this framework, we define the equilibrium by

$$\mathcal{M}(v)=\frac{\exp(-\mathscr{E}(v))}{\displaystyle\int_{\mathbb{R}^N}\exp(-\mathscr{E}(v_\star))\,\mathrm{d}v_\star}.$$

Then, we can work either with linear Boltzmann operators

$$\int\sigma(v,v_\star)\Big(\mathcal{M}(v)f(v_\star)-f(v)\mathcal{M}(v_\star)\Big)\,\mathrm{d}v_\star$$

with σ a positive kernel verifying $\sigma(Rv,Rv_\star)=\sigma(v,v_\star)=\sigma(v_\star,v)$ for any isometry $R\in O(\mathbb{R}^N)$, or with the following Fokker-Planck operator

$$\nabla_v\cdot(a(v)f+\nabla_v f)=\nabla_v\cdot\Big(\mathcal{M}\nabla_v\frac{f}{\mathcal{M}}\Big).$$

However, for such examples motivated by the physics of charged particles, it would be relevant to take into account in (1.1) the effects of some electric field. It induces additional difficulties and these issues are addressed elsewhere [47].

2.2 Diffusion Asymptotics, Hilbert Expansion

Coming back to (1.1), the limit $\varepsilon\to0$ leads to a diffusion equation; precisely f_ε converges to $\rho(t,x)\mathcal{M}(v)$, where ρ satisfies the heat equation

$$\partial_t\rho-\nabla_x\cdot\big(\mathcal{D}\nabla_x\rho\big)=0,\qquad \mathcal{D}=\int_{\mathcal{V}}a(v)\otimes\chi\,\mathrm{d}v,\tag{2.9}$$

where the positivity of the diffusion matrix $\mathcal{D}$ has been established in Lemma 2.1. There are various proofs of such a result, see for instance [6,18]; the analysis includes nonlinear models [3–5,29,39],...

Let us recall that we can guess the result by inserting the Hilbert expansion

$$f_\varepsilon = F^{(0)} + \varepsilon F^{(1)} + \varepsilon^2 F^{(2)} + \dots \tag{2.10}$$

into (1.1). Identifying terms with the same power of ε yields

$$\mathcal{O}(1/\varepsilon) \text{ term:} \qquad Q(F^{(0)}) = 0, \tag{2.11}$$

$$\mathcal{O}(1) \text{ term:} \qquad Q(F^{(1)}) = a(v)\cdot\nabla_x F^{(0)}, \tag{2.12}$$

$$\mathcal{O}(\varepsilon) \text{ term:} \quad Q(F^{(2)}) = \partial_t F^{(0)} + a(v)\cdot\nabla_x F^{(1)}. \tag{2.13}$$

Since $\mathrm{Ker}(Q) = \mathrm{Span}\{\mathcal{M}\}$, (2.11) implies $F^{(0)}(t,x,v) = \rho(t,x)\mathcal{M}(v)$. Then, solvability of (2.12) and (2.13) relies on application of the Fredholm alternative for the operator Q. It follows that $F^{(1)}(t,x,v) = -\chi(v)\cdot\nabla_x\rho(t,x)$ (up to an element of $\mathrm{Ker}(Q)$ which will be irrelevant). Finally, the compatibility condition applied to (2.13) leads to

$$\partial_t \int_{\mathcal{V}} F^{(0)}\,\mathrm{d}v + \nabla_x \cdot \int_{\mathcal{V}} a(v) F^{(1)}\,\mathrm{d}v = 0. \tag{2.14}$$

Coming back to the expression obtained above for $F^{(0)}$ and $F^{(1)}$, we end up with (2.9).

Specializing to Assumption 2.5, we obtain

$$\mathcal{D} = \int_{\mathcal{V}} a(v)\otimes a(v)\ \lambda(|v|)\ M(|v|)\mathrm{d}v.$$

For example, with $a(v) = v$, we have

- For the relaxation operator (2.8) with $\mathcal{M}(v) = 1$ on $\mathbb{S}^{N-1}$, we find

$$\mathcal{D} = \frac{1}{\sigma}\int_{\mathbb{S}^{N-1}} v\otimes v\mathrm{d}v = \frac{1}{N\sigma},$$

- For the relaxation operator (2.8) with $\mathcal{M}(v) = 1$ on $(-1,+1)$ we find

$$\mathcal{D} = \frac{1}{\sigma}\int_{-1}^{1} v^2\mathrm{d}v = \frac{1}{3\sigma}$$

  (remind that $\mathrm{d}v$ is normalized),

- For the isotropic scattering in neutron transport, $\mathcal{V} = \mathbb{S}^{N-1}$ and $\mathcal{M}(v) = 1$, we find (see notation in Section 2.1.2)

$$\mathcal{D} = \frac{1}{N(\beta - \bar{\mu_1}_0)},$$

- For the relaxation operator or the Fokker-Planck operator on $\mathbb{R}^N$ with $\mathcal{M}(v) = (2\pi)^{-N/2}\, e^{-v^2/2}$, we find

$$\mathcal{D} = \frac{1}{\sigma}\int_{\mathbb{R}^N} v\otimes v e^{-v^2/2}\frac{\mathrm{d}v}{(2\pi)^{N/2}} = \frac{1}{\sigma}.$$

2.3 Derivation of the Nonlocal Equation

The derivation is inspired by the Hilbert expansion. We slightly modify the conservation relation (2.14) by introducing a $\varepsilon-$dependent correction. To avoid confusion, let us set up notation. Hereafter, we impose Assumptions 2.1–2.5 We define the following $\varepsilon-$dependent functions

$$F_\varepsilon^{(0)}(t,x,v)=\varrho_\varepsilon(t,x)\ \mathcal{M}(v),\qquad F_\varepsilon^{(1)}(t,x,v)=-\chi(v)\cdot\nabla_x\varrho_\varepsilon(t,x).$$

We remind that $F_\varepsilon^{(1)}$ solves $Q(F_\varepsilon^{(1)})=a(v)\cdot\nabla_x F_\varepsilon^{(0)}$. It remains to derive an evolution equation for ϱ_ε. To this end, we define $G_\varepsilon^{(1)}$ solution of

$$\varepsilon a(v)\cdot\nabla_x G_\varepsilon^{(1)}+G_\varepsilon^{(1)}=F_\varepsilon^{(1)}. \tag{2.15}$$

Then, we obtain a closed equation for ϱ_ε by requiring the pair $(F_\varepsilon^{(0)},G_\varepsilon^{(1)})$ to satisfy the conservation relation

$$\partial_t\int_{\mathcal{V}}F_\varepsilon^{(0)}\,\mathrm{d}v+\nabla_x\cdot\int_{\mathcal{V}}a(v)G_\varepsilon^{(1)}\,\mathrm{d}v=\partial_t\varrho_\varepsilon-\nabla_x\cdot\int_{\mathcal{V}}a(v)\ (\mathbb{I}+\varepsilon a(v)\cdot\nabla_x)^{-1}\big[\chi(v)\cdot\nabla_x\varrho_\varepsilon\big]\,\mathrm{d}v=0. \tag{2.16}$$

In other words, instaed of using the $P1$ approximation $\rho-\chi(v)\cdot\nabla_x\rho$ of f_ε, with $\rho(t,x)$ solution of (2.9), this approach defines an approximated distribution function by

$$\varrho_\varepsilon(t,x)+\varepsilon\left(G_\varepsilon^{(1)}(t,x,v)-\int_{\mathcal{V}}G_\varepsilon^{(1)}(t,x,v_\star)\mathrm{d}v_\star\right).$$

When $\varepsilon=0$, the corrector becomes $G^{(1)}(t,x,v)=-\chi(v)\cdot\nabla_x\rho(t,x)$ and we recover (2.9) by (2.16) which reads

$$\partial_t-\nabla_x\cdot\int_{\mathcal{V}}a(v)\ \chi(v)\cdot\nabla_x\rho(t,x)\mathrm{d}v=0.$$

We have thus introduced a small correction which is intended to retain more microscopic information.

3 A Few Properties of the Nonlocal Equation

3.1 Definition of the Nonlocal Operator

Equation (2.15) can be solved by integrating along the characteristics $x+\tau\varepsilon a(v)$. We get

$$\begin{aligned}G_\varepsilon^{(1)}(t,x,v) &= \int_0^\infty e^{-\tau}F_\varepsilon^{(1)}(t,x-\tau\varepsilon a(v),v)\mathrm{d}\tau\\ &= -\int_0^\infty e^{-\tau}\chi(v)\cdot\nabla_x\varrho_\varepsilon(t,x-\tau\varepsilon a(v))\mathrm{d}\tau.\end{aligned}$$

Based on this expression, we can derive convolution formulas for defining the flux: assuming for instance

$$a(v)=v, \qquad \lambda=1,$$

we obtain

- when $\mathcal{V}=(-1,+1)$ and $\mathcal{M}(v)=1$:

$$\int_{-1}^{+1} a(v)G_\varepsilon^{(1)}\,\mathrm{d}v=-\int_{\mathbb{R}}\partial_x\varrho_\varepsilon(t,y)k_\varepsilon(x-y)\,\mathrm{d}y$$

  with

$$k_\varepsilon(z)=\frac{z^2}{\varepsilon^3}\int_{|z|/\varepsilon}^{\infty}\frac{e^{-\tau}}{\tau^3}\,\mathrm{d}\tau=\frac{z^2}{\varepsilon}\int_{|z|}^{\infty}\frac{e^{-\tau/\varepsilon}}{\tau^3}\,\mathrm{d}\tau.$$

- when $\mathcal{V}=\mathbb{S}^{N-1}$ and $\mathcal{M}(v)=1$:

$$\int_{\mathbb{S}^{N-1}} a(v)G_\varepsilon^{(1)}\,\mathrm{d}v=-\int_{\mathbb{R}^N}k_\varepsilon(x-y)\;\nabla_x\varrho_\varepsilon(t,y)\,\mathrm{d}y$$

  with

$$k_\varepsilon(z)=\frac{e^{-|z|/\varepsilon}}{\varepsilon}\;\frac{z\otimes z}{|z|^{N+1}}.$$

- when $\mathcal{V}=\mathbb{R}^N$ and $\mathcal{M}(v)=e^{-v^2/2}$:

$$\int_{\mathbb{R}^N} a(v)G_\varepsilon^{(1)}\,\mathrm{d}v=-\int_{\mathbb{R}^N}k_\varepsilon(x-y)\;\nabla_x\varrho_\varepsilon(t,y)\,\mathrm{d}y$$

  with

$$k_\varepsilon(z)=\frac{z\otimes z}{\varepsilon}\;\int_0^\infty\frac{\exp(-\frac{\tau}{\varepsilon}-\frac{z^2}{2\tau^2})}{\tau^{N+2}}\,\mathrm{d}\tau.$$

These expressions compare to the empirical formulae derived in [43].

3.2 Computation of the Symbol

We can also obtain interesting formula appealing from the Fourier transform

$$\mathscr{F}(\xi)=\widehat{f}(\xi)=\int_{\mathbb{R}^N}f(x)e^{-ix\cdot\xi}\,\mathrm{d}x.$$

We are led to

$$\widehat{G_\varepsilon^{(1)}}(t,\xi,v)=\frac{\widehat{F_\varepsilon^{(1)}}(t,\xi,v)}{1+i\varepsilon a(v)\cdot\xi}=\frac{-i\chi(v)\cdot\xi}{1+i\varepsilon a(v)\cdot\xi}\;\widehat{\varrho}_\varepsilon(t,\xi).$$

Therefore, we compute the associated flux

$$\int_{\mathcal{V}} a(v)\ \widehat{G_\varepsilon^{(1)}}(t,\xi,v)\,\mathrm{d}v = \int_{\mathcal{V}} a(v)\ \frac{-i\chi(v)\cdot\xi}{1+i\varepsilon a(v)\cdot\xi}\,\mathrm{d}v\ \widehat{\varrho}_\varepsilon(t,\xi).$$

Finally, (2.16) can be interpreted as a pseudo-differential equation

$$\left\{\begin{array}{l} \partial_t \varrho_\varepsilon = -\mathscr{F}^{-1}\Big(\Psi_\varepsilon(\xi)\ \widehat{\varrho}_\varepsilon(t,\xi)\Big), \\ \Psi_\varepsilon(\xi) = -\displaystyle\int_{\mathcal{V}} \frac{a(v)\cdot\xi\ \chi(v)\cdot\xi}{1+i\varepsilon a(v)\cdot\xi}\,\mathrm{d}v. \end{array}\right. \tag{3.1}$$

We write

$$\Psi_\varepsilon(\xi) = -\int_{\mathcal{V}} \frac{a(v)\cdot\xi\ \ \chi(v)\cdot\xi}{1+\varepsilon^2|a(v)\cdot\xi|^2}\,\mathrm{d}v + i\varepsilon\int_{\mathcal{V}} \chi(v)\cdot\xi\ \frac{|a(v)\cdot\xi|^2}{1+\varepsilon^2|a(v)\cdot\xi|^2}\,\mathrm{d}v$$

and we remark that the imaginary part vanishes when Assumption 2.5-i), and ii) hold (since χ is odd in such a case). Let us state the main properties of this Fourier operator.

Proposition 3.1. Suppose that Assumptions 2.1–2.5 are satisfied. Then, the following assertions hold:
i) We have

$$\begin{aligned} \Psi_\varepsilon(\xi) &= \int_{\mathcal{V}} \frac{|a(v)\cdot\xi|^2}{1+\varepsilon^2|a(v)\cdot\xi|^2}\ \lambda(|v|)\mathcal{M}(|v|)\mathrm{d}v \\ &= \frac{1}{\varepsilon^2}\left(\int_{\mathcal{V}} \lambda(|v|)\mathcal{M}(|v|)\mathrm{d}v - \int_{\mathcal{V}} \frac{\lambda(|v|)\mathcal{M}(|v|)}{1+\varepsilon^2|a(v)\cdot\xi|^2}\ \mathrm{d}v\right) \end{aligned}$$

which is real and satisfies $0\le\Psi_\varepsilon(\xi)\le\|\lambda(|v|)M\|_{L^1(\mathcal{V})}/\varepsilon^2$.
ii) For $0<\varepsilon'<\varepsilon$, $0\le\Psi_\varepsilon(\xi)\le\Psi_{\varepsilon'}(\xi)\le\mathcal{D}\xi\cdot\xi=\int_{\mathcal{V}}|a(v)\cdot\xi|^2\ \lambda(|v|)\mathcal{M}(|v|)\mathrm{d}v$.
iii) For any fixed $\varepsilon>0$, we have

$$|\Psi_\varepsilon(\xi)-\mathcal{D}\xi\cdot\xi| \le \varepsilon^2|\xi|^4\ \int_{\mathcal{V}}|a(v)|^4\lambda(|v|)\mathcal{M}(v)\mathrm{d}v.$$

If, furthermore for any $0<R<\infty$, and $\omega\in\mathbb{S}^{N-1}$ we have $\mathrm{meas}\{v\in\mathcal{V}\cap B(0,R),\ a(v)\cdot\omega=0\}=0$, then

$$\lim_{|\xi|\to\infty}\Psi_\varepsilon(\xi)=\frac{1}{\varepsilon^2}\int_{\mathcal{V}}\lambda(|v|)\mathcal{M}(v)\mathrm{d}v.$$

iv) For any fixed $\xi\in\mathbb{R}^N$, we have

$$\lim_{\varepsilon\to0}\Psi_\varepsilon(\xi)=\mathcal{D}\xi\cdot\xi.$$

In some circumstances, the function $\Psi_\varepsilon(\xi)$ can be computed explicitly:

Proposition 3.2. Let us consider cases where $a(v)=v$, $\lambda=1=\sigma$.
i) When $\mathcal{M}(v)=1$, and $\mathrm{d}v$ is the (normalized) Lebesgue measure we have

$$\begin{cases} \text{For } \mathcal{V}=(-1,+1) \text{ or } \mathcal{V}=\mathbb{S}^2: & \Psi_\varepsilon(\xi)=\dfrac{1}{\varepsilon^2}\Big(1-\dfrac{\arctan(\varepsilon|\xi|)}{\varepsilon|\xi|}\Big), \\ \text{For } \mathcal{V}=\mathbb{S}^1: & \Psi_\varepsilon(\xi)=\dfrac{1}{\varepsilon^2}\Big(1-\dfrac{1}{\sqrt{1+\varepsilon^2\xi^2}}\Big). \end{cases}$$

ii) When $\mathcal{V}\subset\mathbb{R}^N$ is endowed with the Lebesgue measure and it can be recast as $\mathcal{I}\times\mathbb{S}^{N-1}$, with $\mathcal{I}$ a measurable set of $\mathbb{R}$, assuming $\mathcal{M}(v)=M(|v|)$, we get

$$\begin{cases} \text{For } N=3: & \Psi_\varepsilon(\xi)=\dfrac{4\pi}{\varepsilon^2}\displaystyle\int_{\mathcal{I}}\Big(1-\dfrac{\arctan(\varepsilon|\xi|r)}{\varepsilon|\xi|r}\Big)\,M(r)r^{N-1}\mathrm{d}r, \\ \text{For } N=2: & \Psi_\varepsilon(\xi)=\dfrac{2\pi}{\varepsilon^2}\displaystyle\int_{\mathcal{I}}\Big(1-\dfrac{1}{\sqrt{1+\varepsilon^2|\xi|^2r^2}}\Big)\,M(r)r\mathrm{d}r, \\ \text{For } N=1: & \Psi_\varepsilon(\xi)=\displaystyle\int_{\mathcal{I}}\dfrac{r^2\xi^2}{1+\varepsilon^2\xi^2r^2}M(r)\mathrm{d}r. \end{cases}$$

We shall discuss a more intricate example with a function $v\mapsto a(v)$ which takes into account relativistic effects later on. It is worth discussing in details the two velocity model (2.6), with $a(v)=v$. It is convenient to rewrite the problem by means of the distribution function $f_\varepsilon^\pm(t,x)$ of particles with velocity ±1. With this slight change of notation, we obtain the following system

$$\partial_t f_\varepsilon^\pm \pm \frac{1}{\varepsilon}\partial_x f_\varepsilon^\pm = \frac{1}{\varepsilon^2}\Big(\rho_\varepsilon - f_\varepsilon^\pm\Big) = \mp\frac{f_\varepsilon^+ - f_\varepsilon^-}{2\varepsilon^2} \tag{3.2}$$

with

$$\rho_\varepsilon = \frac{f_\varepsilon^+ + f_\varepsilon^-}{2}.$$

We introduce the current

$$J_\varepsilon = \frac{f_\varepsilon^+ - f_\varepsilon^-}{2\varepsilon}.$$

In this particular case the moment system satisfied by $(\rho_\varepsilon, J_\varepsilon)$ is closed and completely equivalent to (3.2). We get

$$\begin{cases} \partial_t\rho_\varepsilon + \partial_x J_\varepsilon = 0, \\ \varepsilon^2\partial_t J_\varepsilon + \partial_x\rho_\varepsilon = -J_\varepsilon. \end{cases} \tag{3.3}$$

We can remark that

$$\partial_x J_\varepsilon = -\partial_{xx}^2\rho_\varepsilon - \varepsilon^2\partial_t\partial_x J^\varepsilon = -\partial_{xx}^2\rho_\varepsilon + \varepsilon^2\partial_{tt}^2\rho_\varepsilon$$

so that ρ_ε satisfies the damped wave equation

$$\varepsilon^2\partial_{tt}^2\rho_\varepsilon + \partial_t\rho_\varepsilon = \partial_{xx}^2\rho_\varepsilon.$$

Writing the system (3.3) with $\varepsilon=0$, one obtains the Fick relation

$$J=-\partial_x\rho$$

and thus the conservation law leads to the heat equation

$$\partial_t\rho=-\partial_x J=\partial^2_{xx}\rho.$$

The standard Chapman-Enskog expansion consists in writing

$$\begin{array}{rcl}\partial_t\rho_\varepsilon & = & \partial_x(-J_\varepsilon)=\partial_x\big(\partial_x\rho_\varepsilon+\varepsilon^2\partial_t J_\varepsilon\big)\\ & = & \partial^2_{xx}\rho_\varepsilon-\varepsilon^2\partial_x\partial_t\big(\partial_x\rho_\varepsilon+\varepsilon^2\partial_t J_\varepsilon\big).\end{array}$$

It could be tempting to get rid of the $\mathcal{O}(\varepsilon^4)$ terms in this formula; it yields

$$\partial_t(1+\varepsilon^2\partial^2_{xx})\rho_\varepsilon=\partial^2_{xx}\rho_\varepsilon$$

but we realize readily that this approximated model is not a well posed problem.

In our approach, we define

$$\widehat{G^\pm_\varepsilon}=\pm\frac{1\pm\mathrm{i}\varepsilon\xi}{1+\varepsilon^2\xi^2}\;\mathrm{i}\xi\;\widehat{\varrho}_\varepsilon$$

and then the approximated flux is given by

$$\widehat{J}_\varepsilon=\frac{1}{2}(\widehat{G^+_\varepsilon}-\widehat{G^-_\varepsilon})=\frac{\mathrm{i}\xi\;\widehat{\varrho}_\varepsilon}{1+\varepsilon^2\xi^2}.$$

In other words the Fick relation is replaced by the elliptic equation

$$(1-\varepsilon^2\partial^2_{xx})J_\varepsilon=-\partial_x\varrho_\varepsilon.$$

The corresponding symbol reads $\Psi_\varepsilon(\xi)=\xi^2/(1+\varepsilon^2\xi^2)$. The inverse Fourier transform yields

$$\mathscr{F}^{-1}\Psi_\varepsilon(x)=\frac{1}{\varepsilon^2}\Big(\delta_{x=0}-\frac{1}{2\varepsilon}e^{-|x|/\varepsilon}\Big).$$

Accordingly, ϱ_ε satisfies the integro-differential equation

$$\partial_t\varrho_\varepsilon(t,x)=-\frac{1}{\varepsilon^2}\varrho_\varepsilon(t,x)+\frac{1}{2\varepsilon^3}\int_{\mathbb{R}}e^{-|x-y|/\varepsilon}\varrho_\varepsilon(t,y)\,\mathrm{d}y.$$

Of course, we can simply write

$$\partial_t\varrho_\varepsilon=\partial_x(1-\varepsilon^2\partial^2_{xx})^{-1}\partial_x\varrho_\varepsilon,$$

that is also

$$\partial_t(1-\varepsilon^2\partial^2_{xx})\varrho_\varepsilon=\partial^2_{xx}\varrho_\varepsilon.$$

Proof of Proposition 3.1. The claims i) and ii) as well as iv) are obvious consequences of the formula that defines Ψ_ε. Next, we compute

$$\begin{aligned} 0 \le \mathcal{D}\xi\cdot\xi - \Psi_\varepsilon(\xi) &= \int_{\mathcal{V}} |a(v)\cdot\xi|^2 \frac{\varepsilon^2|a(v)\cdot\xi|^2}{1+\varepsilon^2|a(v)\cdot\xi|^2}\lambda(|v|)\mathcal{M}(v)\,\mathrm{d}v \\ &\le \varepsilon^2|\xi|^4\int_{\mathcal{V}}|a(v)|^4\lambda(|v|)\mathcal{M}(v)\,\mathrm{d}v. \end{aligned}$$

Now, let us set $\xi = r\omega$, $r=|\xi|$, $\omega\in\mathbb{S}^{N-1}$. We check that

$$\Psi_\varepsilon(r\omega) = \int_{\mathcal{V}} \frac{|a(v)\cdot\omega|^2}{1/r^2+\varepsilon^2|a(v)\cdot\omega|^2}\,\lambda(|v|)\mathcal{M}(v)\,\mathrm{d}v \xrightarrow[r\to\infty]{} \frac{1}{\varepsilon^2}\int_{\mathcal{V}} \mathbf{1}_{|a(v)\cdot\omega|>0}\lambda(|v|)\mathcal{M}(v)\,\mathrm{d}v,$$

but the integrand equals $\lambda(|v|)\mathcal{M}(v)$ a.e. with the additional assumption on $(\mathcal{V},\mathrm{d}v)$. (Note that in general the limit depends on the direction ω as shown with a 4 velocities example in dimension 2).

Proof of Proposition 3.2. Of course, the proof uses spherical coordinates $v=r\Omega$, $r=|v|\in\mathcal{I}$, $\Omega = v/|v|\in\mathbb{S}^{N-1}$, which yields the following expressions

$$\Psi_\varepsilon(\xi) = C\int_{\mathcal{I}} I(\xi,r)\; M(r)r^{N-1}\mathrm{d}r$$

where the constant C and the function $r\mapsto I(\xi,r)$ depend on the space dimension. It turns out that we are led to compute the integrals (where we have set $|\xi|\cos(\theta)=\xi\cdot\Omega$ to parametrize the sphere)

$$\begin{aligned} \text{For } N\ge 3: \qquad I(\xi,r) &= \int_0^\pi \frac{\xi^2r^2\cos^2(\theta)}{1+\varepsilon^2\xi^2r^2\cos^2(\theta)}\,\sin(\theta)\mathrm{d}\theta \\ &= \frac{1}{\varepsilon^2}\int_{-\varepsilon|\xi|r}^{+\varepsilon|\xi|r}\frac{z^2}{1+z^2}\,\frac{\mathrm{d}z}{\varepsilon|\xi|r} = \frac{2}{\varepsilon^2}\Big(1-\frac{\arctan(\varepsilon|\xi|r)}{\varepsilon|\xi|r}\Big) \\ \text{For } N=2: \qquad I(\xi,r) &= \int_0^{2\pi}\frac{\xi^2r^2\cos^2(\theta)}{1+\varepsilon^2|\xi|^2r^2\cos^2(\theta)}\,\mathrm{d}\theta = \frac{2\pi}{\varepsilon^2} - \frac{4}{\varepsilon^2}\int_0^{\pi/2}\frac{\mathrm{d}\theta}{1+\varepsilon^2|\xi|^2r^2\cos^2(\theta)} \\ &= \frac{2\pi}{\varepsilon^2} - \frac{4}{\varepsilon^2}\int_0^\infty\frac{\mathrm{d}u}{1+\varepsilon^2|\xi|^2r^2+u^2} = \frac{2\pi}{\varepsilon^2} - \frac{2\pi}{\varepsilon^2\sqrt{1+\varepsilon^2|\xi|^2r^2}}. \end{aligned}$$

The case $\mathcal{V}=(-1,+1)$ follows the same computation.

3.3 Consistency with the Diffusion Approximation

Let us make a couple of comments on Proposition 3.1. At first, (3.1) leads to

$$\widehat{\varrho_\varepsilon}(t,\xi) = e^{-\Psi_\varepsilon(\xi)t}\widehat{\varrho_{\mathrm{Init}}}(\xi) \tag{3.4}$$

where $\varrho_{\mathrm{Init}}(x)=\int_{\mathcal{V}} f_{\mathrm{Init}}(x,v)\,\mathrm{d}v$ is the initial condition for (3.1), assumed independent on ε. Then, Proposition 3.1-i) guarantees the well-posedness in $L^2(\mathbb{R}^N)$, together with the dissipation property

$$\frac{\mathrm{d}}{\mathrm{d}t}\int_{\mathbb{R}^N}\varrho_\varepsilon^2(t,x)\,\mathrm{d}x \le 0. \tag{3.5}$$

(Actually any space derivative of the unknown is dissipated in L^2 norm.) With Proposition 3.1-ii) and iii) we understand that (3.1) corresponds to a diffusion equation for small frequencies but to a mere ODE for large frequencies. Finally, iv) implies that (3.1) is consistent with the diffusion approximation since letting ε go to 0 yields, for fixed ξ

$$\widehat{\varrho_\varepsilon}(t,\xi) \xrightarrow[\varepsilon\to 0]{} e^{-\mathcal{D}\xi\cdot\xi t}\widehat{\varrho_{\rm Init}}(\xi).$$

This implies (by a simple application of the Lebesgue theorem) that ϱ_ε tends to the solution of (2.9). More precisely, we have, for any $0\le t\le T<\infty$,

$$\begin{aligned}\|\varrho_\varepsilon(t)-\rho(t)\|^2_{L^2(\mathbb{R}^N)} &= \int_{\mathbb{R}^N} e^{-2\Psi_\varepsilon(\xi)t}\,|1-e^{-(\mathcal{D}\xi\cdot\xi-\Psi_\varepsilon(\xi))t}|^2\,|\widehat{\rho_{\rm Init}}(\xi)|^2{\rm d}\xi\\ &\le \int_{\mathbb{R}^N}|1-e^{-(\mathcal{D}\xi\cdot\xi-\Psi_\varepsilon(\xi))T}|^2\,|\widehat{\rho_{\rm Init}}(\xi)|^2{\rm d}\xi \xrightarrow[\varepsilon\to 0]{} 0.\end{aligned}$$

Furthermore, we have

$$\begin{aligned}\|\varrho_\varepsilon(t)-\rho(t)\|^2_{L^2(\mathbb{R}^N)} &\le \int_{\mathbb{R}^N}|(\mathcal{D}\xi\cdot\xi-\Psi_\varepsilon(\xi))T|^2|\widehat{\rho_{\rm Init}}(\xi)|^2{\rm d}\xi\\ &\le \varepsilon^2\,T^2\times\int_{\mathcal{V}}|a(v)|^4\lambda(|v|)\mathcal{M}(v){\rm d}v\times\int_{\mathbb{R}^N}|\xi|^4\,|\widehat{\rho_{\rm Init}}|^2{\rm d}\xi.\end{aligned}$$

Summarizing, we obtain the following statement.

Theorem 3.1. *For any $\rho_{\rm Init}\in L^2(\mathbb{R}^N)$, there exists a unique solution $\varrho_\varepsilon\in C^0(\mathbb{R}^+;L^2(\mathbb{R}^N))$ of* (2.16). *As ε goes to 0, ϱ_ε converges to ρ, solution of* (2.9) *in $C^0([0,T];L^2(\mathbb{R}^N))$ for any $0<T<\infty$. If $\rho_{\rm Init}\in H^2(\mathbb{R}^N)$, the convergence holds with a rate $\mathcal{O}(\varepsilon)$.*

Remark 3.1. Note also that ϱ_ε formally fulfills the mass conservation since $\widehat{\varrho_\varepsilon}(t,0)=\widehat{\rho_{\rm Init}}(0)=\int_{\mathbb{R}^N}\rho_{\rm Init}(x){\rm d}x$.

4 Approximation of the Nonlocal Equation

This Section is concerned with numerical purposes; precisely we address the question of the computation of the solution of (2.16). A natural attempt would be to use the equivalent formulation (3.1) and a simple explicit Euler scheme

$$\varrho_\varepsilon^{n+1}-\varrho_\varepsilon^n=-\Delta t\;\mathscr{F}^{-1}\big(\Psi_\varepsilon(\xi)_\varepsilon^n\big)$$

where the right hand side is evaluated by means of Fast Fourier Transform. However, such a spectral approach might lead to technical difficulties when the resolution of the kinetic equation is part of a bigger problem involving a coupling with other PDEs or simply when considering non periodic boundary conditions. It also leads to the standard difficulty of truncating the Fourier variable. It motivates to search for approximations of $\Psi_\varepsilon(\xi)$ that allow a treatment by usual PDEs approximation techniques. Furthermore, we wish to design a fully macroscopic model; in particular we do not want to go back to a kinetic framework that would involve the additional variable v, by solving the coupled equations (2.15)-(2.16) defining ϱ and G.

4.1 Approximation of the Pseudo-Differential Symbol

Our goal is to replace $\Psi_\varepsilon(\xi)$ by a rational function $P_\varepsilon/Q_\varepsilon(\xi)$ so that we shall replace the pseudodifferential equation (3.1) by

$$\partial_t Q_\varepsilon(i\partial_x)\varrho_\varepsilon = P_\varepsilon(i\partial_x)\varrho_\varepsilon$$

where now the differential operators $P_\varepsilon(i\partial_x)$ and $Q_\varepsilon(i\partial_x)$ can be treated by finite differences, finite elements or finite volumes approaches.

Remark 4.1. For the two velocity model, the function $\Psi_\varepsilon(\xi) = \xi^2/(1+\varepsilon^2\xi^2)$ already has the desired form which directly yields

$$\partial_t(1-\varepsilon^2\partial_{xx}^2)\varrho_\varepsilon = \partial_{xx}^2\varrho_\varepsilon.$$

It can be treated for instance with the scheme

$$\varrho_i^{n+1} - \varepsilon^2\frac{\varrho_{i+1}^{n+1}-2\varrho_i^{n+1}+\varrho_{i-1}^{n+1}}{\Delta x^2} = \varrho_i^n + (\Delta t-\varepsilon^2)\frac{\varrho_{i+1}^n-2\varrho_i^n+\varrho_{i-1}^n}{\Delta x^2}.$$

Note that even if the scheme is based on the explicit Euler scheme, it requires the inversion of a linear system.

To be specific, we restrict the discussion to the framework

$$a(v)=v, \qquad \mathcal{V}=\mathbb{S}^2 \text{ or } (-1+1), \qquad \mathcal{M}(v)=1$$

detailed in Proposition 3.2-i). The strategy can be extended to other situations, as discussed in the Examples above, but the formula could become much more intricate and not as explicit as in this simple case. The diffusion equation which corresponds to the small mean free path limit reads

$$\partial_t\rho - \frac{1}{3}\Delta_x\rho = 0 \tag{4.1}$$

while

$$\Psi_\varepsilon(\xi) = \frac{1}{\varepsilon^2}\Big(1-\frac{\arctan(\varepsilon|\xi|)}{\varepsilon|\xi|}\Big).$$

To start with, we can use the Taylor series associated to the function $\psi(z)=(1-\arctan(z)/z)$, namely

$$\sum_{n=0}^{\infty} a_n\, z^n, \qquad a_0=0, \quad a_{2k}=\frac{(-1)^{k+1}}{2k+1}, \quad a_{2k+1}=0.$$

This is known to usually provide a useless approximation, but it serves as a basis to define the Padé approximant which gives a good rational approximation. We define

$$P(z)=p_0+p_1z^1+\cdots+p_Mz^M, \qquad Q(z)=1+q_1z^1+\cdots+q_Mz^M.$$

so that

$$Q(z)\psi(z)-P(z)=\mathcal{O}(|z|^{2M+1}) \qquad \text{as } z\to 0.$$

Indeed, since we have remarked that $\Psi_\varepsilon(\xi)$ behaves like a constant for large ξ's it is relevant to select P and Q with the same higher degree. Accordingly, $(p_0,\dots,p_M,q_1,\dots,q_M)$ satisfies the linear system

$$\begin{cases} \text{For } m\in\{0,\dots,M\}, & \displaystyle\sum_{n=0}^{m} a_n\, q_{m-n}-p_m=0, \\ \text{For } m\in\{M+1,\dots,2M\}, & \displaystyle\sum_{n=0}^{M} a_{m-n}\, q_n=0 \end{cases}$$

For $M=2$ this yields the following approximation

$$\frac{z^2/3}{1+3z^2/5}.$$

Accordingly, we approach $\Psi_\varepsilon(\xi)$ by

$$\frac{|\xi|^2/3}{1+3\varepsilon^2|\xi|^2/5}.$$

This would lead to the following definition of the approximate equation

$$\partial_t\Big(1-\varepsilon^2\frac{3}{5}\Delta_x\Big)\varrho_\varepsilon=\frac{1}{3}\Delta_x\varrho_\varepsilon.$$

However, this approximation is not satisfactory since it misses the right behavior of $\psi(z)$ for large z's. This is usual in the approximation of pseudo-differential operators, where a range of frequencies is privileged, see for instance the applications of such techniques for defining absorbing boundary conditions [22, 23]. Therefore, we modify the definition of the approximant by imposing the correct behavior at infinity: we require

$$\psi(z)-P/Q(z)=\mathcal{O}(|z|^{2M}) \quad \text{as } z\to 0, \quad \text{and} \quad \psi(z)-P/Q(z)=\mathcal{O}(1/z) \quad \text{as } z\to+\infty.$$

For $M=2$ this yields the following approximation

$$\frac{z^2/3}{1+z^2/3}.$$

This would lead to the following definition of the approximate equation

$$\partial_t\Big(1-\frac{\varepsilon^2}{3}\Delta_x\Big)\varrho_\varepsilon=\frac{1}{3}\Delta_x\varrho_\varepsilon. \tag{4.2}$$

For $M=4$, we are led to

$$P(z)=\frac{1}{3}z^2+\frac{38}{245}z^4, \qquad Q(z)=1+\frac{33}{49}z^2+\frac{38}{245}z^4.$$

Therefore the equation reads

$$\partial_t\Big(1-\varepsilon^2\frac{33}{49}\,\Delta_x+\varepsilon^4\frac{38}{245}\Delta_x^2\Big)\varrho_\varepsilon=\Big(\frac{1}{3}\Delta_x+\varepsilon^2\frac{38}{245}\Delta_x^2\Big)\varrho_\varepsilon.$$

However, a high order approximation is certainly more difficult to treat numerically and does not always provide significantly better results. Fig. 1 shows graphs of the various approximation of the symbol $\Psi_\varepsilon(\xi)$; in particular we note that high order approximations present larger discrepancies for the intermediate frequencies.

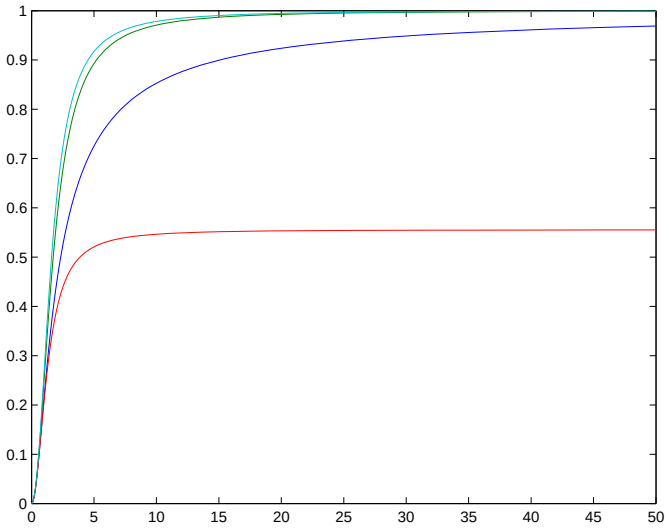

Figure 1: Graph of the function Ψ (blue curve, $\varepsilon=1$) vs. its approximation: $(x^2/3)/(1+3x^2/5)$ (red curve), $x^2/3/(1+x^2/3)$ (green curve), $(x^2/3+38x^4/245)/(1+33x^2/49+38x^4/245)$ (cyan curve).

It is remarkable that, at least in dimension 1, the approximate model (4.2) can be obtained by using a different reasoning, based on a quadrature formula for evaluating the integral that defines the symbol Ψ_ε. Some hints is this direction can be found in [51], where the convolution operator derived on physical grounds is approached in this way to recover a formula proposed in [42]. We consider a finite number of positive weights $(\omega_1,...,\omega_M)$ and velocities $(v_1,...,v_M)$ in $(-1,+1)$ and we approach integrals $\int_{-1}^{+1}\phi(v)\,\mathrm{d}v$ by using a finite number of points: $\sum_{i=1}^M\omega_i\phi(v_i)$. At least it is natural to require the preservation of the fundamental properties of the velocity space which govern the diffusion regime, that is

$$\sum_{i=1}^M\omega_i=1,\qquad\sum_{i=1}^M\omega_i\,v_i=0,\qquad\sum_{i=1}^M\omega_i\,v_i^2=\frac{1}{3}.$$

Specializing to a 2 velocities approximations, $M=2$, these constraints naturally lead to the following definition of weights and velocities

$$\omega_1=\omega_2=1/2, \qquad v_1=-v_2=1/\sqrt{3}.$$

Accordingly, we are led to approach the symbol $\Psi_\varepsilon(\xi)=\int_{-1}^{+1}\frac{v^2\xi^2}{1+\varepsilon^2v^2\xi^2}\mathrm{d}v$ by

$$2\times\frac{1}{2}\frac{\xi^2/3}{1+\varepsilon^2\xi^2/3},$$

and we recover that way the model (4.2).

4.2 Further examples

Let us detail similar manipulations for the Gaussian case in dimension three. According to Proposition 3.2-ii) the symbol reads

$$\Psi_\varepsilon(\xi)=\frac{4\pi}{\varepsilon^2}\int_0^\infty\Big(1-\frac{\arctan(\varepsilon|\xi|r)}{\varepsilon|\xi|r}\Big)e^{-r^2/2}\mathrm{d}r.$$

The Taylor expansion leads to

$$\frac{2\sqrt{2}}{3\sqrt{\pi}}\xi^2-\frac{6\sqrt{2}}{5\sqrt{\pi}}\varepsilon^2\xi^4.$$

We therefore identify the coefficients of P and Q:

$$p_0=p_1=q_1=0, \quad p_2=\frac{2\sqrt{2}}{3\sqrt{\pi}}.$$

We also have $\lim_{\xi\to\infty}\Psi_\varepsilon(\xi)=\frac{2\sqrt{2}}{\sqrt{\pi}\varepsilon^2}$ which gives $q_2=\varepsilon^2/3$. The Padé approximant of Ψ_ε is

$$\frac{2\sqrt{2}}{\sqrt{\pi}}\frac{\xi^2/3}{1+\varepsilon^2\xi^2/3}$$

Figure 2 compares the Padé approximant to the symbol.

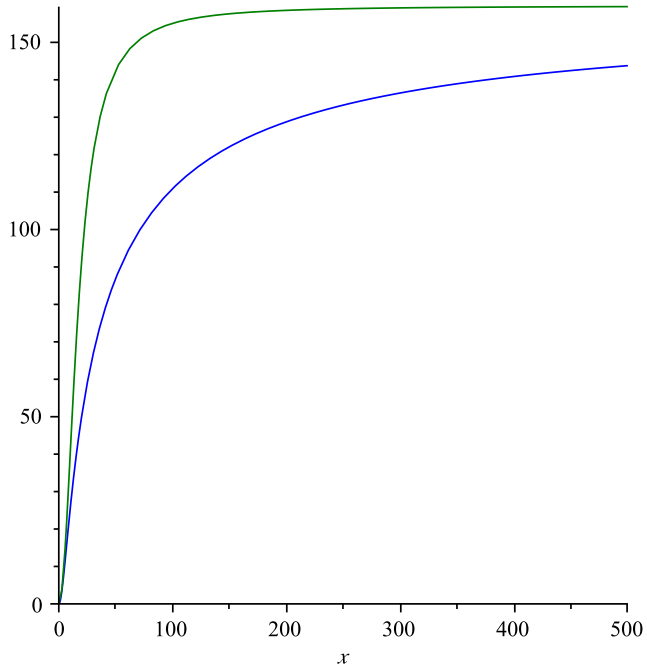

Figure 2: Graph of the function Ψ in blue vs the Padé approximant in green for $\varepsilon = 10^{-1}$

We can also present some computations for the relativistic case where

$$a(v) = \frac{v}{\sqrt{1+v^2}}, \qquad \mathcal{M}(v) = e^{-(\sqrt{1+v^2}-1)}.$$

In dimension three, the function Ψ_ε becomes

$$\Psi_\varepsilon(\xi) = \int_{\mathbb{R}^3} \frac{(v\cdot\xi)^2 \frac{1}{1+v^2}}{1+\varepsilon^2 \frac{(v\cdot\xi)^2}{1+v^2}} e^{-(\sqrt{1+v^2}-1)}\,\mathrm{d}v.$$

Some algebraic computations lead to

$$\Psi_\varepsilon(\xi) = \frac{4\pi}{\varepsilon^2}\int_0^\infty \left(1 - \frac{\arctan \frac{|\xi| r\varepsilon}{\sqrt{1+r^2}}}{\frac{|\xi| r\varepsilon}{\sqrt{1+r^2}}}\right) r^2 e^{-(\sqrt{1+r^2}-1)}\,\mathrm{d}r.$$

Let us compute the Padé approximant with the correct behavior at infinity as $\dfrac{P(\xi)}{Q(\xi)}$ where $P(\xi) = p_0 + p_1\xi + p_2\xi^2$ and $Q(\xi) = 1 + q_1\xi + q_2\xi^2$ The 4^{th} order Taylor expansion of $\Psi_\varepsilon(\xi)$ is

$$\frac{4\pi}{\varepsilon^2}\left(\int_0^\infty \frac{1}{3}\frac{r^4 \mathrm{e}^{-\sqrt{1+r^2}+1}}{1+r^2}\mathrm{d}r\xi^2\varepsilon^2 - \int_0^\infty \frac{1}{5}\frac{r^6 \mathrm{e}^{-\sqrt{1+r^2}+1}}{(1+r^2)^2}\mathrm{d}r\xi^4\varepsilon^4\right)$$

We find $p_0 = p_1 = 0$ and $p_2 = 4\pi \int_0^\infty 1/3 \dfrac{r^4 \mathrm{e}^{-\sqrt{1+r^2}+1}}{1+r^2} \mathrm{d}r$.
The limit of Ψ_ε as $\xi \to \infty$ is $\dfrac{4\pi}{\varepsilon^2} \int_0^\infty r^2 \mathrm{e}^{-\sqrt{1+r^2}+1} dr$. We therefore find $q_1 = 0$ and $q_2 = \frac{p_2}{\lim_{\xi\to\infty} \Psi_\varepsilon(\xi)}$ so that

$$q_2 = \frac{\varepsilon^2}{3} \frac{\displaystyle\int_0^\infty \frac{r^4 \mathrm{e}^{-\sqrt{1+r^2}+1}}{1+r^2} dr}{\displaystyle\int_0^\infty r^2 \mathrm{e}^{-\sqrt{1+r^2}+1} dr}$$

The Padé approximant is therefore

$$\frac{P(\xi)}{Q(\xi)} = \left(1 + \frac{\varepsilon^2}{3} \frac{\displaystyle\int_0^\infty \frac{r^4 \mathrm{e}^{-\sqrt{1+r^2}+1}}{1+r^2} \mathrm{d}r}{\displaystyle\int_0^\infty r^2 \mathrm{e}^{-\sqrt{1+r^2}+1} \mathrm{d}r} \xi^2 \right)^{-1} \times \frac{4\pi}{3} \int_0^\infty \frac{r^4 \mathrm{e}^{-\sqrt{1+r^2}+1}}{1+r^2} \mathrm{d}r \xi^2$$

which is approximately

$$\frac{P(\xi)}{Q(\xi)} = \frac{15.38539180\ \xi^2}{1 + 0.2772004346\ \varepsilon^2\ \xi^2}.$$

Figure 3 compares the Padé approximant to the symbol.

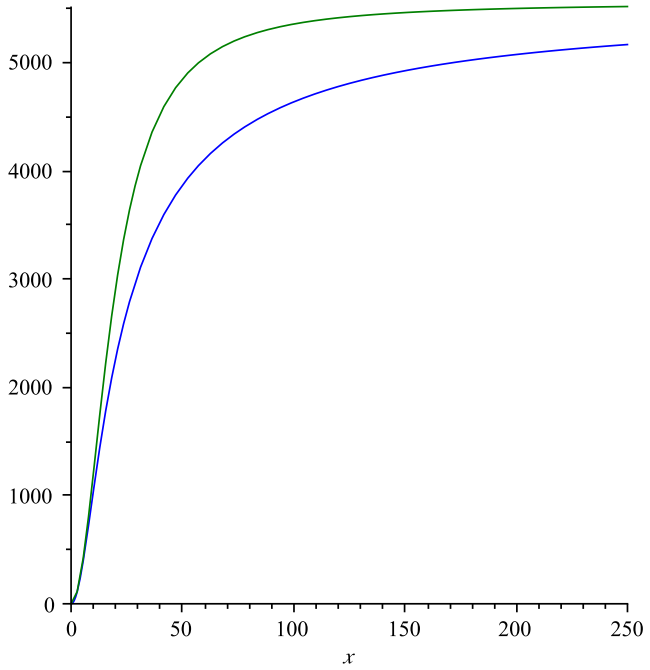

Figure 3: Graph of the function Ψ in blue vs the Padé approximant in green for $\varepsilon = 10^{-1}$

4.3 Numerical Scheme for the Approximate Equation

We focus our discussion on the numerical scheme to the simplest model (4.2) in the one-dimension framework. We treat the space derivative with the usual 3-points finite difference scheme and for the time derivative, we use the $\theta-$scheme

$$\begin{aligned}\rho_j^{n+1}-\Big(\theta\frac{\Delta t}{\Delta x^2}+\frac{\varepsilon^2}{\Delta x^2}\Big)\frac{\rho_{j+1}^{n+1}-2\rho_j^{n+1}+\rho_{j-1}^{n+1}}{3}\\ =\rho_j^n+\Big((1-\theta)\frac{\Delta t}{\Delta x^2}-\frac{\varepsilon^2}{\Delta x^2}\Big)\frac{\rho_{j+1}^n-2\rho_j^n+\rho_{j-1}^n}{3}\end{aligned} \tag{4.3}$$

The amplification factor reads

$$\frac{1-\frac{2}{3\Delta x^2}\big((1-\theta)\Delta t-\varepsilon^2\big)+\frac{2}{3\Delta x^2}\cos(\xi\Delta x)\big((1-\theta)\Delta t-\varepsilon^2\big)}{1+\frac{2}{3\Delta x^2}\big(\theta\Delta t+\varepsilon^2\big)-\frac{2}{3\Delta x^2}\cos(\xi\Delta x)\big(\theta\Delta t+\varepsilon^2\big)}$$

and we conclude that the scheme is stable under the CFL condition

$$1-2\theta-\frac{2\varepsilon^2}{\Delta t}\leq\frac{3\Delta x^2}{2\Delta t}.$$

In particular, the scheme is unconditionally stable for the implicit scheme $\theta=1$ and for the Crank-Nicolson case $\theta=1/2$ which can be expected to reach 2nd order accuracy with respect to Δt and Δx. Anyway, the scheme is always stable under the standard parabolic CFL: $2\Delta t/3\Delta x^2\leq 1$. Similar conclusion applies if the equation is treated by a finite element approach. As a matter of fact, we can also check that the scheme preserves the following energy conservations associated to (4.2)

$$\begin{aligned}&\frac{1}{2}\frac{\mathrm{d}}{\mathrm{d}t}\left(\int\varrho^2\mathrm{d}x+\frac{\varepsilon^2}{3}\int|\partial_x\varrho|^2\mathrm{d}x\right)+\frac{1}{3}\int|\partial_x\varrho|^2\mathrm{d}x=0,\\ &\frac{1}{2}\frac{\mathrm{d}}{\mathrm{d}t}\int|\partial_x\varrho|^2\mathrm{d}x+\int\Big(|\partial_t\varrho|^2+\varepsilon^2|\partial_{tx}^2\varrho|^2\Big)\mathrm{d}x=0.\end{aligned}$$

4.4 Numerical Results

At first, we compare the solutions of the heat equation (4.1) with various approximations devised above in the periodic framework. It allows to compute the solutions directly by FFT methods and thus to discuss the role of the nonlocal approximated model, without any further numerical approximations. Results are displayed in Fig. 4 and 5 for the discontinuous initial datum

$$\rho_{\mathrm{Init}}(x)=\mathbf{1}_{(-1/4,-1/8)\cup(1/8,1/4)}(x)+\frac{1}{2}\mathbf{1}_{(-1/8,1/8)}(x). \tag{4.4}$$

The solution is computed on the domain $(-1,1)$ and is discretized with 4096 Fourier modes. The smoothing of the profile is reduced and delayed when using the approximated models, which furthermore preserve a higher L^∞ norm. Of course, this is completely clear by a dispersion analysis: high frequencies are rapidly damped by the heat

equation, while they are conserved by the pseudo-differential equation since the symbol tends to a constant for large frequencies. As expected, the Padé approximation provides a solution in between the solution of the heat equation and those of the pseudo-differential equation with the symbol Ψ_ε but it is able to preserve the sharp profiles. In Fig. 6, we add to the previous comparison simulations with the standard second order Padé approximant without correction at infinity and the fourth order approximation. It confirms that increasing the order of approximation does not change significantly the result. In regular region, the standard approximation seems to have better behavior, but the global L^∞ error compared to computation made with the symbol is less accurate.

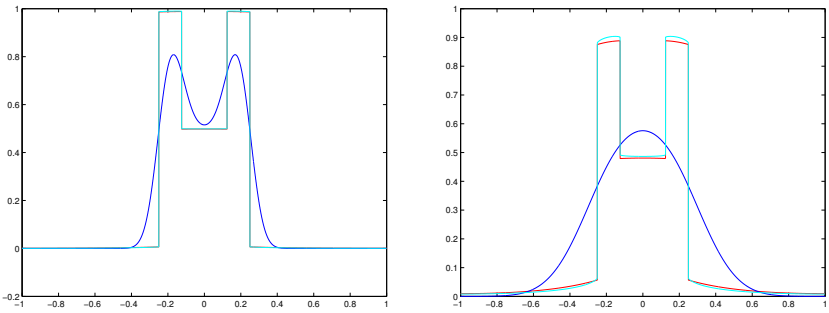

(a) $\varepsilon = 0.5$, $T = 0.005$ (b) $\varepsilon = 0.5$, $T = 0.05$

(c) $\varepsilon = 0.5$, $T = 0.1$ (d) $\varepsilon = 0.5$, $T = 0.5$

Figure 4: Periodic case: computation by FFT for $\varepsilon = 0.5$ and several final time: In blue the solution of the heat equation, in cyan the solution with the Fourier multiplier $\Psi_\varepsilon(\xi) = \frac{1}{\varepsilon^2}(1 - \arctan(\varepsilon|\xi|)/(\varepsilon|\xi|))$, in red the solution with the Padé approximant $\xi^2/3/(1+\varepsilon^2\xi^2/3)$.

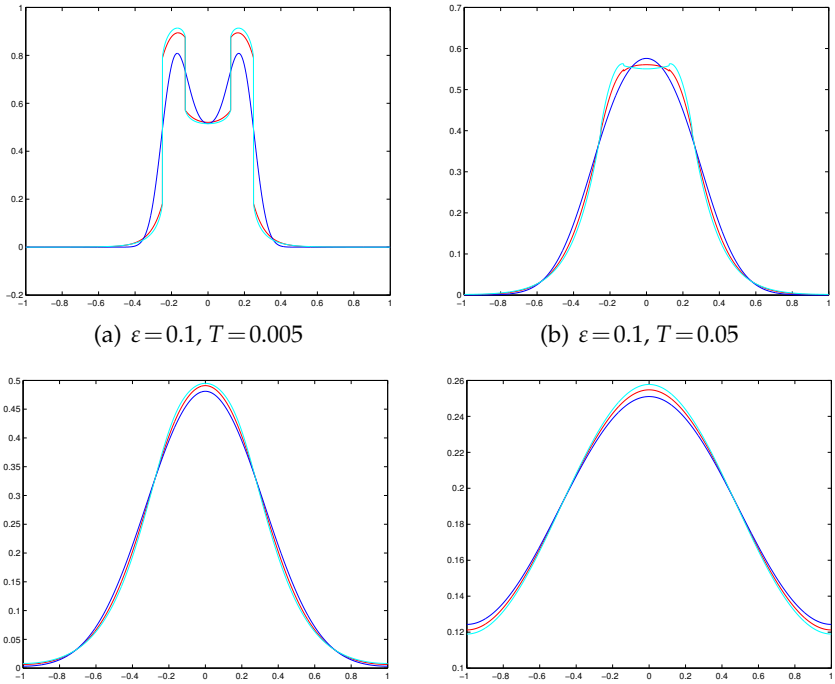

(a) $\varepsilon = 0.1$, $T = 0.005$ (b) $\varepsilon = 0.1$, $T = 0.05$

(c) $\varepsilon = 0.1$, $T = 0.1$ (d) $\varepsilon = 0.1$, $T = 0.5$

Figure 5: Periodic case: computation by FFT for $\varepsilon = 0.1$ and several final time: In blue the solution of the heat equation, in cyan the solution with the Fourier multiplier $\Psi_\varepsilon(\xi) = \frac{1}{\varepsilon^2}(1 - \arctan(\varepsilon|\xi|)/(\varepsilon|\xi|))$, in red the solution with the Padé approximant $\xi^2/3/(1+\varepsilon^2\xi^2/3)$.

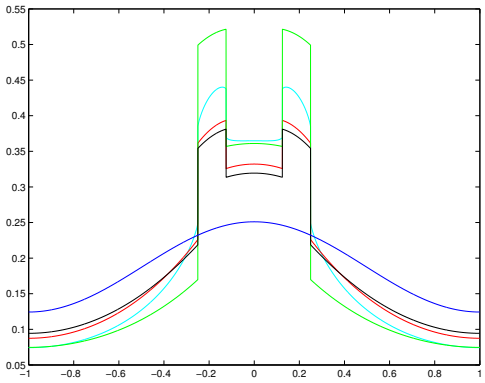

Figure 6: Periodic case: computation by FFT for $\varepsilon = 0.5$ and final time $T = 0.5$: The solution of the heat equation (blue), using the Fourier multiplier (cyan), the approximant $x^2/3/(1+x^2/3)$ (red), $(x^2/3)/(1+3x^2/5)$ (green) and $(x^2/3+38x^4/245)/(1+33x^2/49+38x^4/245)$ (black).

We perform similar simulations in a bounded domain with Neumann boundary conditions and using the $\theta-$scheme (4.3) (with $\theta = 1/2$) with 1000 discretization points. The time step is chosen to be 10^{-3}. Fig. 7 compares the results obtained by solving the heat equation (4.1) and (4.2). The conclusion of the periodic case applies: the approximate model has less smoothing effects, and the discrepancies disappear as time becomes larger, the solutions having the same asymptotic trend to equilibrium. Anyway, as ε goes to 0, the discrepancies are sensible for shorter time, and disappear rapidly.

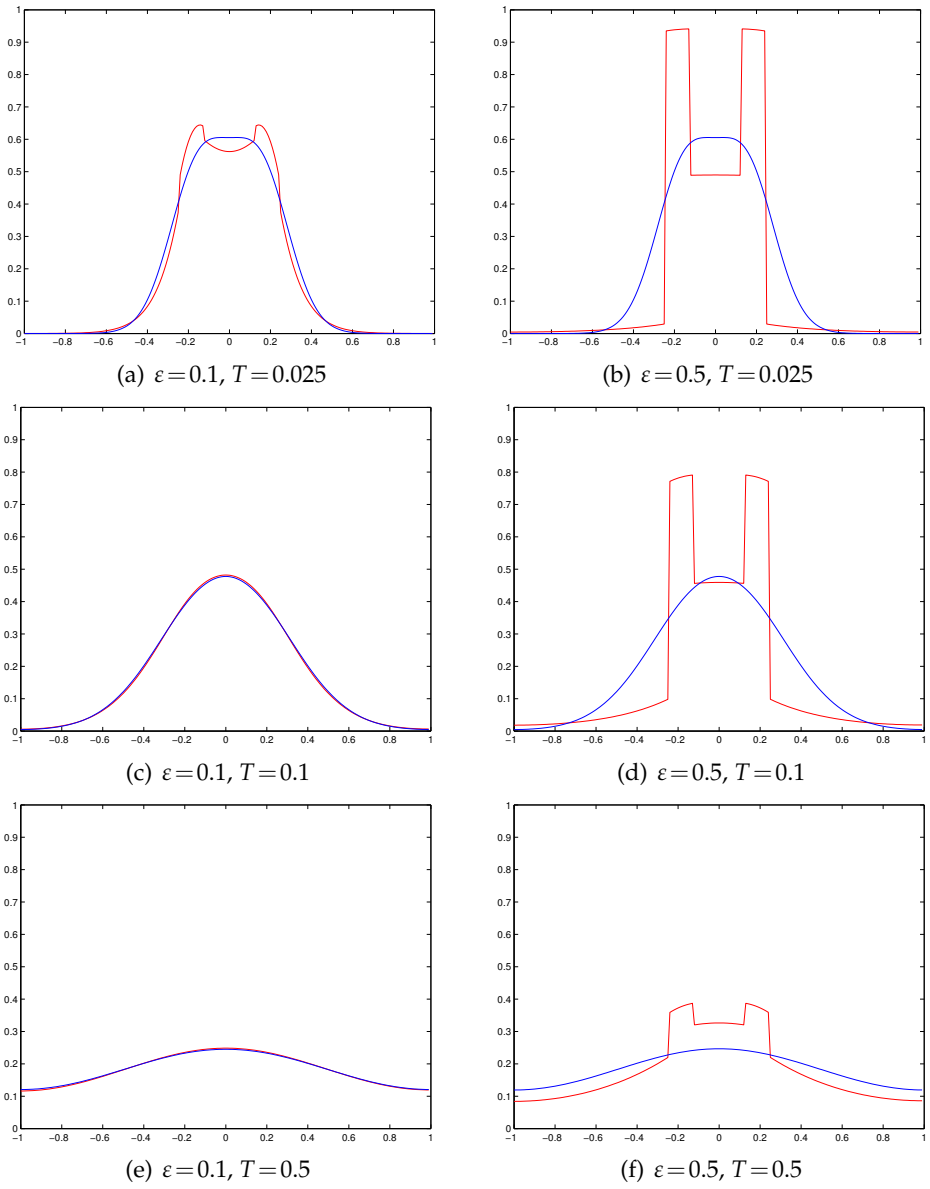

(a) $\varepsilon = 0.1$, $T = 0.025$ (b) $\varepsilon = 0.5$, $T = 0.025$

(c) $\varepsilon = 0.1$, $T = 0.1$ (d) $\varepsilon = 0.5$, $T = 0.1$

(e) $\varepsilon = 0.1$, $T = 0.5$ (f) $\varepsilon = 0.5$, $T = 0.5$

Figure 7: Neumann boundary conditions: computation by the Cranck-Nicolson scheme for several ε and final time: In blue the solution of the heat equation, in red the solution with the Padé approximant $\xi^2/3/(1+\varepsilon^2\xi^2/3)$.

Second, it is natural to ask also for a comparison with a direct simulation of the kinetic equation

$$\partial_t f + \frac{v}{\varepsilon}\partial_x f = \frac{1}{\varepsilon^2}\left(\int_{-1}^{+1} f(v_\star)\,\mathrm{d}v_\star - f\right)$$

that the pseudo-differential equation (4.2) is intended to approach. We keep in mind that we are only interested in the evolution of the macroscopic quantity $\int_{-1}^{+1} f(v_\star)\mathrm{d}v_\star$. To this end, we simulate the kinetic equation by using an involved numerical scheme which reduces artificial viscosity effect. We use the P-Weno introduced in [14] which is based on the Weno interpolation procedure. Of course such a simulation becomes very costly as ε goes to 0, due to the CFL condition that imposes $\Delta t \lesssim \varepsilon \Delta x$. We present on Figures 8 and 9 the evolution of the solution of nonlocal, kinetic and heat model with initial datum (4.4) respectively for $\varepsilon = 0.5$ and $\varepsilon = 0.1$.

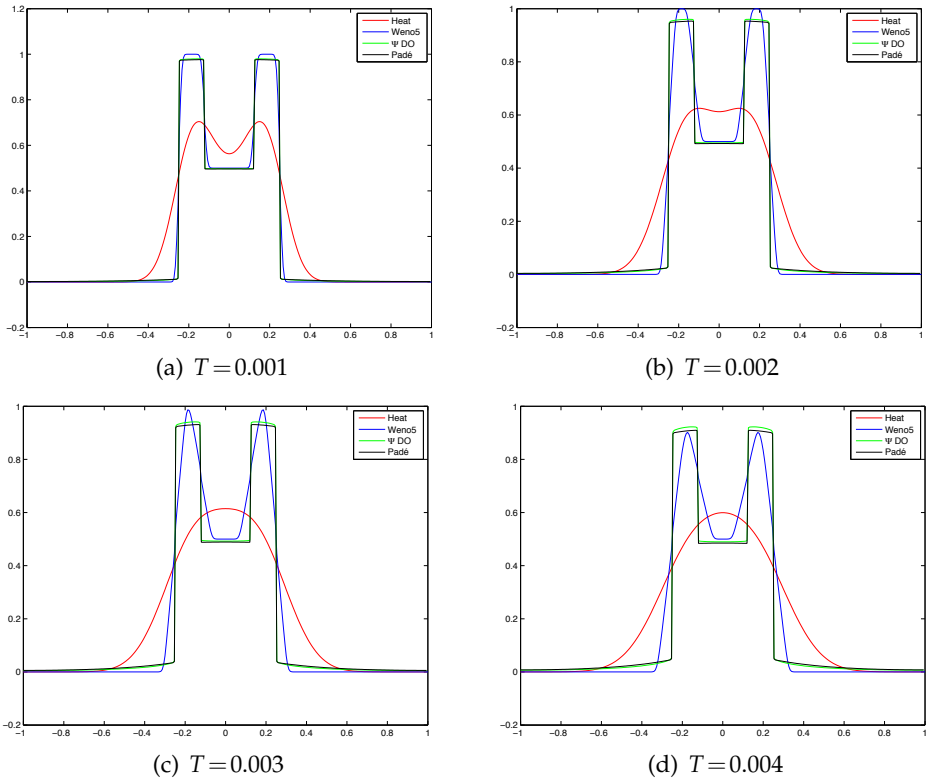

(a) $T = 0.001$ (b) $T = 0.002$

(c) $T = 0.003$ (d) $T = 0.004$

Figure 8: Comparison between heat, pseudodifferential and kinetic equations for $\varepsilon = 0.5$ and several final time

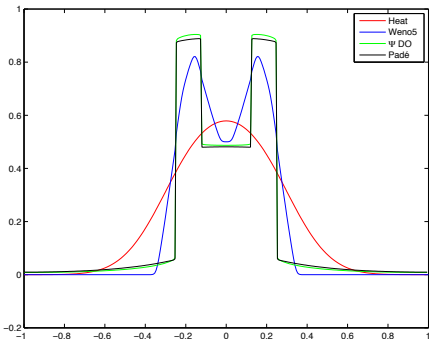

(e) $T = 0.005$

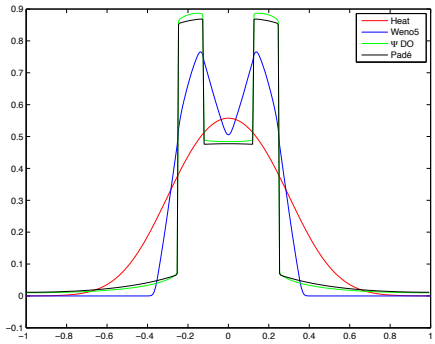

(f) $T = 0.006$

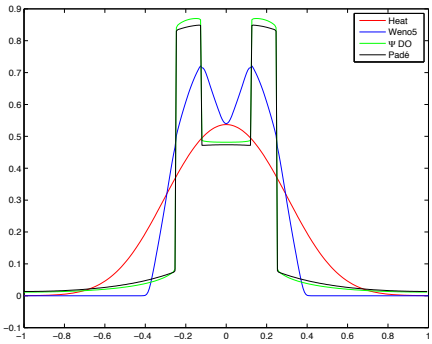

(g) $T = 0.007$

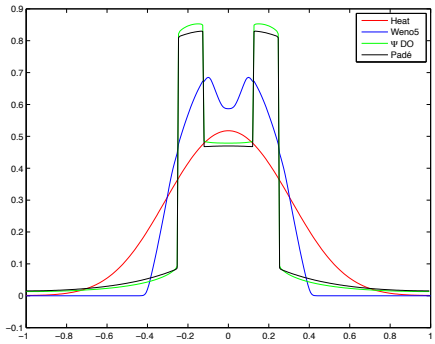

(h) $T = 0.008$

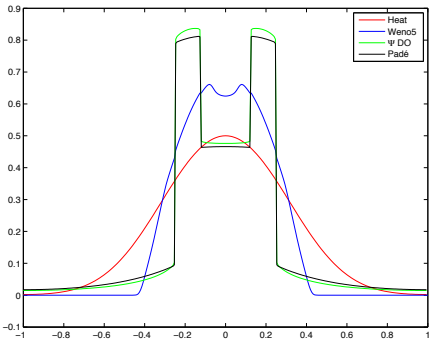

(i) $T = 0.009$

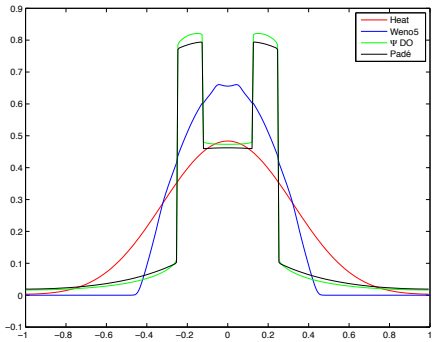

(j) $T = 0.01$

Figure 8: Continued

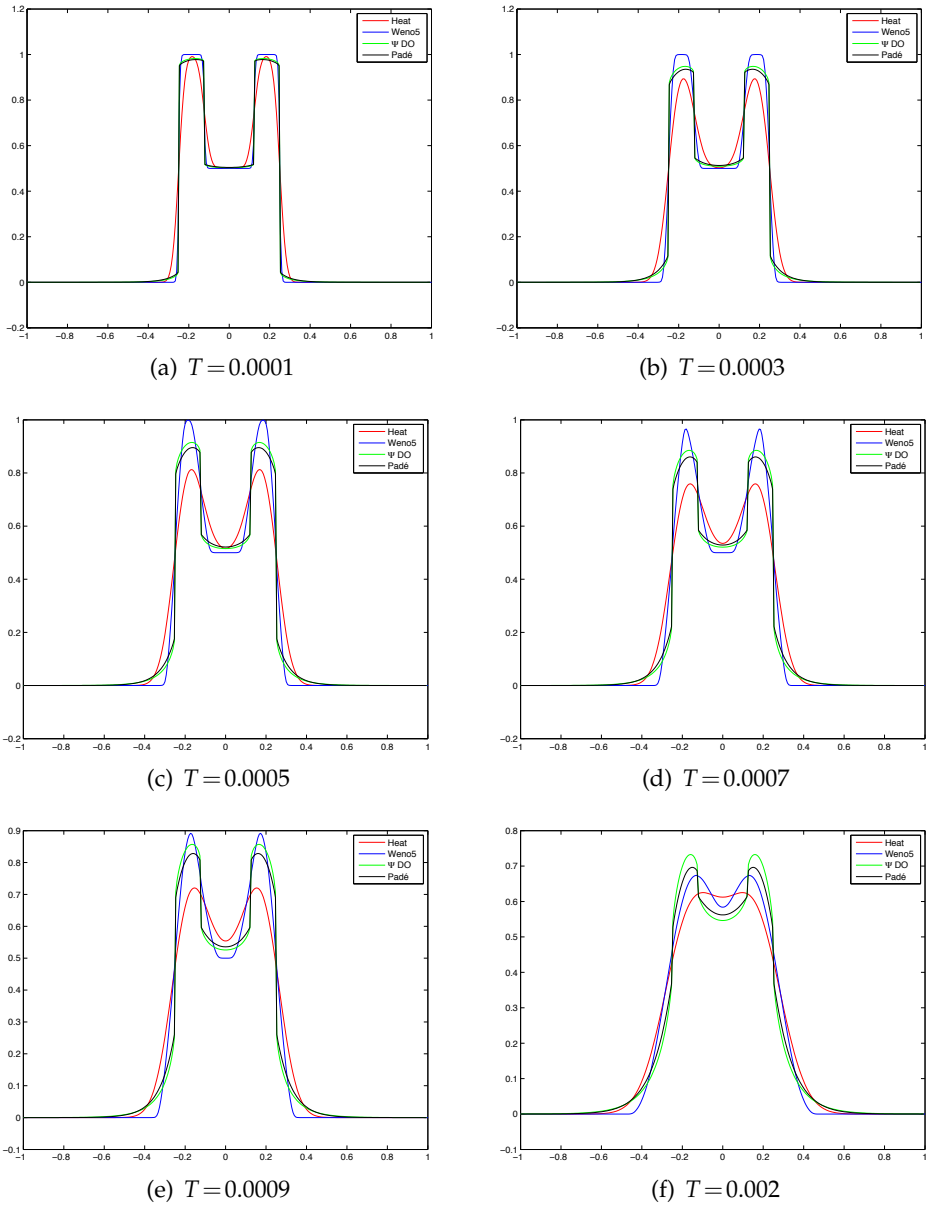

(a) $T = 0.0001$ (b) $T = 0.0003$

(c) $T = 0.0005$ (d) $T = 0.0007$

(e) $T = 0.0009$ (f) $T = 0.002$

Figure 9: Comparison between heat, pseudodifferential and kinetic equations for $\varepsilon = 0.1$ and several final time

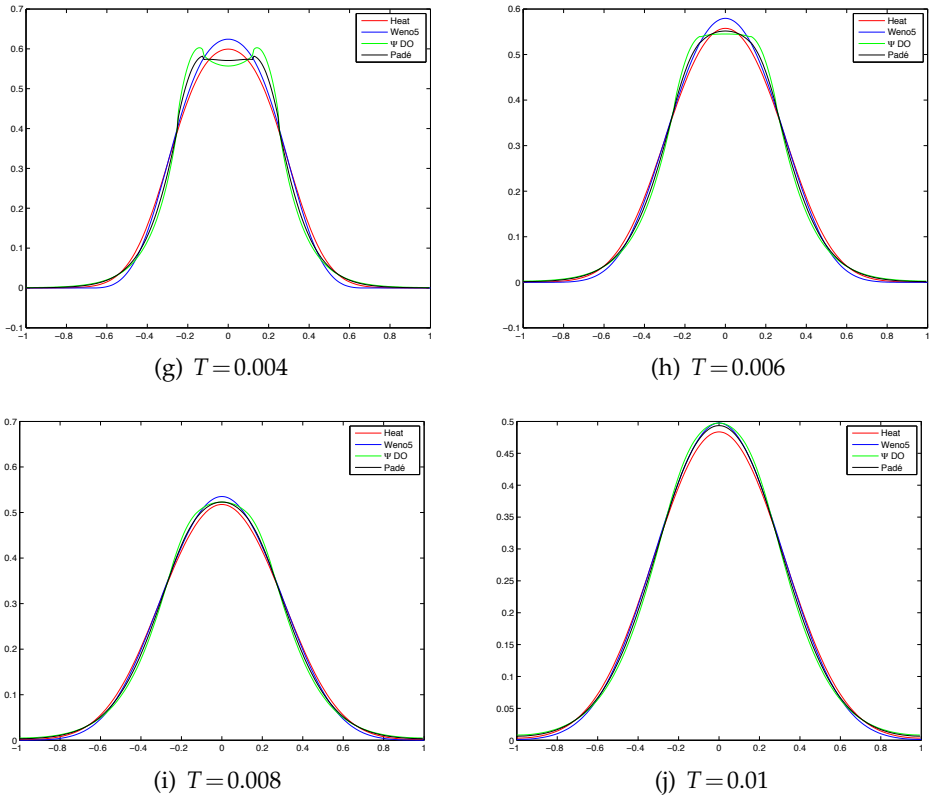

(g) $T = 0.004$ (h) $T = 0.006$

(i) $T = 0.008$ (j) $T = 0.01$

Figure 9: Continued

We clearly observe that the behavior of nonlocal model is with a good agreement for small times with the kinetic equation whereas the heat equation gives rapidly diffusive solutions. At a long time scales, like it is anticipated with the theoretical results, nonlocal and kinetic solutions converge to the solution of the heat equation. Concerning the in-between times, clearly the nonlocal model misses some diffusive properties. As already remarked in [24] about Fokker-Planck simulations, the comparison is not as satisfactory as expected. We can summarize the results as follows: for very short time, the agreement between the pseudo-differential model and the full kinetic model is good, while the heat equation immediately produces an overly smoothed profile, but it rapidly degrades: sharp gradients of density are smoothed faster with the kinetic model (and the amplitude of this effect is such that it does not come from numerical diffusion). Of course, for very long time, these discrepancies disappear since all the models have the same asymptotic trend. The interplay between the largest frequencies present in the data, the mean free path ε and the final time of simulation is very intricate and definitely deserve further analysis, which is beyond the scope of the present work.

5 Applications

As said above, the nonlocal model, or rather its approximation, is quite easy to implement and it provide cheap and decent results. Hence, it is worth discussing some possible adaptations to more complex models. In particular, we shall see that it can be adapted to non linear models, and to complex systems where the kinetic equation is coupled to hydrodynamics equations. This is typically the situation which occur in plasma physics [1, 24, 42, 43, 45, 51, 57], and we shall go back to this issue elsewhere, see [47]. Here, we present instead a few applications in radiative transfer. In both cases, the non local model can be interesting by its ability to preserve sharp gradient on short time and to remain computable for a reasonable cost.

5.1 Nonlinear Grey Radiative Transfer Equation

In what follows, the variable v lies in $\mathbb{S}^2$ or $\mathcal{V}=(-1,+1)$ so that we set

$$\Psi_\varepsilon(\xi)=\frac{1}{\varepsilon^2}\Big(1-\frac{\arctan(\varepsilon|\xi|)}{\varepsilon|\xi|}\Big).$$

We consider the equation

$$\partial_t f_\varepsilon+\frac{v}{\varepsilon}\cdot\nabla_x f_\varepsilon=\frac{1}{\varepsilon^2}\sigma(\rho_\varepsilon)(\rho_\varepsilon-f_\varepsilon),\qquad \rho_\varepsilon(t,x)=\int_{\mathcal{V}} f_\varepsilon(t,x,v)\,\mathrm{d}v,$$

with a function $\sigma:(0,+\infty)\to\mathbb{R}^+$, for instance $\sigma(\rho)=\rho^\alpha$, $|\alpha|<1$. This nonlinear model is introduced in [5] as a caricature of systems arising in radiative transfer, assuming that the material temperature and the radiation temperature have already equilibrated; it contains most of the analytical difficulties of the physical equations. We refer to [3, 5, 29, 39] for the analysis of the asymptotic regime $\varepsilon\to 0$: we can establish the convergence of f_ε to ρ solution of the nonlinear diffusion equation (Rosseland approximation)

$$\partial_t\rho-\frac{1}{3}\Delta_x F(\rho)=0,\qquad F(z)=\int_0^z\frac{\mathrm{d}u}{\sigma(u)}.$$

Reproducing the previous developments leads to the following non local and non linear equation

$$\partial_t\varrho_\varepsilon=-\mathscr{F}^{-1}\Big(\Psi_\varepsilon(\xi)\,\widehat{F(\varrho_\varepsilon)}\Big).$$

The proposed approximation method would be, at the lowest order,

$$\partial_t(1-\varepsilon^2\Delta_x/3)\varrho=\frac{1}{3}\Delta_x F(\varrho).$$

5.2 Radiation coupled to Hydrodynamics

The nonlocal approximation can be applied also when dealing with systems of equations where the kinetic equation describing the radiative energy is coupled to fluid equations describing the evolution of a surrounding gas, interacting through energy exchanges. The fluid is described by its density n, velocity u and total energy E. In what follows, we denote $e=E-u^2/2$ the internal energy and we shall assume that the pressure is given by the constitutive law

$$p=(\gamma-1)ne, \tag{5.1}$$

with $\gamma=C_p/C_v>1$ the adiabatic constant of the gas. Besides, the temperature θ of the gas (material temperature) is given by

$$e=\frac{R}{\gamma-1}\theta \tag{5.2}$$

with R the perfect gas constant. The photons are subject to two kind of interaction phenomena: emission-absorption and scattering. Accordingly, these phenomena lead to the following expression of the interaction operator

$$Q=\sigma_s\Big(\int_{\mathcal{V}} f\,\mathrm{d}v-f\Big)+\sigma_a\Big(\theta^4-f\Big)$$

where $\sigma_{s,a}$ are positive coefficients characterizing scattering and absorption/emission respectively. We adopt here two simplifying assumptions:

- Firstly, we restrict to a grey model where the unknowns and coefficients do not depend on the frequency variable. The unknown $f(t,x,v)$ is interpreted as a radiative intensity: the integral $\frac{1}{c}\int_{\Omega\times O} f(t,x,v)\mathrm{d}v\mathrm{d}x$, with c denoting the light speed, gives the energy at time t corresponding to photons evolving at time t in the domain Ω and following a direction within a solid angle in $O\subset \mathbb{S}^{N-1}=\mathcal{V}$. The grey model is already an approximation since it is obtained by averaging over frequencies the frequency-dependent equation and furthermore the derivation involves a suitable definition of averaged opacities $\sigma_{s,a}$.
- Secondly, we also assume that the opacities do not depend on the temperature θ, which would introduce further nonlinearities (the extension to variable absorption-emission coefficient σ_a is however straightforward).

Then, the dynamics is governed by the following set of equations:

$$\begin{cases} \partial_t n+\nabla_x\cdot(nu)=0, \\ \partial_t(nu)+\nabla_x\cdot(nu\otimes u+p)=0 \\ \partial_t(nE)+\nabla_x\cdot((nE+p)u)=-\displaystyle\int_{\mathcal{V}} Q\mathrm{d}v \end{cases} \tag{5.3}$$

coupled to

$$\frac{1}{c}\partial_t f+v\cdot\nabla_x f=Q. \tag{5.4}$$

It is worth remarking that the system conserves the total energy

$$\frac{\mathrm{d}}{\mathrm{d}t}\left(\int nE\,\mathrm{d}x+\frac{1}{c}\int\int_{\mathcal{V}} f\,\mathrm{d}v\,\mathrm{d}x\right)=0.$$

This is a quite simplified framework: for instance momentum exchanges are neglected as well as Doppler corrections that however can induce important contributions (proportional to u/c) in the asymptotic regimes. We refer to [40,44] for further details on the modeling issues, and to [10, 27] for mathematical analysis. We mention also [2, 20, 52, 56] for interesting applications to combustion phenomena. We distinguish two relevant asymptotic regimes, corresponding to the following rescaling:

$$\begin{array}{ll}\text{Equilibrium Regime:} & c\to\dfrac{1}{\varepsilon}\gg 1,\quad \sigma_a\to\dfrac{\sigma_a}{\varepsilon},\quad \sigma_s\to\sigma_s;\\ \text{Non-Equilibrium Regime:} & c\to\dfrac{1}{\varepsilon}\gg 1,\quad \sigma_a\to\sigma_a,\quad \sigma_s\to\dfrac{\sigma_s}{\varepsilon}.\end{array}$$

In the former case, absorption/emission is the leading phenomena and the temperature of radiation relaxes to the temperature of the gas: $f\simeq\rho(t,x)=\theta^4$. The limit system reads

$$\begin{cases}\partial_t n+\nabla_x\cdot(nu)=0,\\ \partial_t(nu)+\nabla_x\cdot(nu\otimes u+p)=0,\\ \partial_t(nE+\theta^4)+\nabla_x\cdot((nE+p)u)=\dfrac{1}{3\sigma_a}\Delta_x\theta^4.\end{cases}$$

The last equation expresses the balance of the total energy which is in this regime nE (material energy) + θ^4 (radiative energy). Applying the approximation procedure, we replace the energy equation by

$$\partial_t(nE+\theta^4)+\nabla_x\cdot((nE+p)u)=-\frac{1}{\sigma_a}\mathscr{F}^{-1}\Big(\Psi_\varepsilon(\xi)\ \mathscr{F}(\theta^4)\Big).$$

In the non-equilibrium regime, the distribution f still relaxes to an equilibrium which does not depend on the variable v, but the temperature of the radiation (that is $\rho^{1/4}$) differs from the temperature θ of the fluid. This is due to the fact that here scattering dominates over absorption/emission phenomena. The limit equations read

$$\begin{cases}\partial_t n+\nabla_x\cdot(nu)=0,\\ \partial_t(nu)+\nabla_x\cdot(nu\otimes u+p)=0,\\ \partial_t(nE)+\nabla_x\cdot((nE+p)u)=\sigma_a(\rho-\theta^4),\end{cases}\tag{5.5}$$

coupled to the following diffusion equation for the radiation energy

$$\partial_t\rho-\frac{1}{3\sigma_s}\Delta_x\rho=\sigma_a(\theta^4-\rho).\tag{5.6}$$

A further approximation which is often used in practice consists in assuming in (5.6) that $\sigma_a \simeq 1/(3\sigma_s) := \eta^{-1} \gg 1$ so that the time derivative is dropped in (5.6): then, (5.5) is coupled to the simple elliptic equation

$$-\Delta_x \rho = \theta^4 - \rho. \tag{5.7}$$

Applying our approximation procedure replaces (5.6) by

$$\partial_t \rho = -\frac{1}{\sigma_s} \mathscr{F}^{-1}\Big(\Psi_\varepsilon(\xi)\ \mathscr{F}\rho\Big) + \sigma_a(\theta^4 - \rho), \tag{5.8}$$

or its stationary variant. We wish to investigate numerically this asymptotics and see how the nonlocal term modifies the behavior of the solution of the limit equations.

5.3 Numerical Scheme for Radiative Hydrodynamics in the Non equilibrium Regime

In this Section, we are concerned with the non equilibrium regime which is thus described by the system

$$\begin{cases} \partial_t n + \nabla_x \cdot (nu) = 0, \\ \partial_t (nu) + \nabla_x \cdot (nu \otimes u + p) = 0 \\ \partial_t (nE) + \nabla_x \cdot ((nE + p)u) = -\sigma_a(\rho - \theta^4), \\ \partial_t f + \dfrac{v}{\varepsilon} \cdot \nabla_x f = \dfrac{\sigma_s}{\varepsilon^2}(\rho - f) + \sigma_a(\theta^4 - f), \end{cases} \tag{5.9}$$

with $\rho(t,x) = \int_{\mathcal{V}} f(t,x,v)\,\mathrm{d}v$. The difficulties that make a direct simulation non affordable can be summarized as follows:

- The radiative intensity $f(t,x,v)$ depends on the additional variable v compared to the hydrodynamic fields (n,u,E),
- The small parameter $\varepsilon > 0$ makes the characteristic speed of the system (v/ε vs. u and the sound speed) very different; it induces severe stability constraints,
- There are also stiff (zeroth order) terms in the right hand side of the equations.

Therefore, based on asymptotic analysis arguments, it is interesting to replace the coupled hydrodynamic/kinetic system (5.9) by a reduced system having only macroscopic unknowns (i. e. depending on (t,x) only). The extreme situation corresponds to $\varepsilon = 0$ and is given by the system (5.5)–(5.6) satisfied by (n,u,E) and the radiative energy ρ. As said in the Introduction, many systems have been proposed, usually based on some moment closures, to describe intermediate regimes, see in particular [21] for closures based on entropy minimization and [53] for adapted truncation of spherical harmonics expansions, and the references therein.

In what follows we go back to the system obtained with the non local approximation and we describe numerical strategies to solve the problem

$$\begin{cases} \partial_t n + \nabla_x \cdot (nu) = 0, \\ \partial_t (nu) + \nabla_x \cdot (nu \otimes u + p) = 0, \\ \partial_t (nE) + \nabla_x \cdot ((nE+p)u) = \sigma_a(\rho - \theta^4), \\ \eta \partial_t \rho = -\dfrac{1}{\sigma_s} \mathscr{F}^{-1}\Big(\Psi_\varepsilon(\xi)\ \mathscr{F}\rho\Big) + \sigma_a(\theta^4 - \rho). \end{cases} \tag{5.10}$$

Note that all the stiffness is embodied into the pseudo-differential term. With $\eta = 1$, $\varepsilon > 0$ it corresponds to (5.5), (5.8). Letting $\varepsilon \to 0$, we obtain (5.5)–(5.6) while $\eta \to 0$ yields (5.5) coupled to (5.7) or its nonlocal approximation. In fact, as described above, we shall deal with a Padé approximation $P_\varepsilon(\xi)/Q_\varepsilon(\xi)$ of the symbol $\Psi_\varepsilon(\xi)$ since it is amenable to a simpler numerical treatment. For the sake of simplicity, we describe the scheme by restricting ourselves to the one-dimension framework. The numerical scheme we propose for (5.10) is based on a first order splitting in time. Namely, if we assume that the different needed quantities are known at time t_0, we compute the solution at time $t = t_0 + \Delta t$ according to the scheme

initial conditions $n(t_0)$, $u(t_0)$, $E(t_0)$ and $\rho(t_0)$

Step 1

Solve for $t \in [t_0, t_0 + \Delta t]$

$$\begin{cases} \partial_t \bar{n} + \partial_x(\bar{n}\bar{u}) = 0, \\ \partial_t \bar{n}\bar{u} + \partial_x(\bar{n}\bar{u}\bar{u} + \bar{p}) = 0, \\ \partial_t(\bar{n}\bar{E}) + \partial_x((\bar{n}\bar{E} + \bar{p})\bar{u}) = 0, \\ \eta \partial_t \bar{\rho} = 0, \end{cases}$$

with $\bar{n}(t_0) = n(t_0)$, $\bar{u}(t_0) = u(t_0)$, $\bar{E}(t_0) = E(t_0)$ and $\bar{\rho}(t_0) = \rho(t_0)$.

Step 2

Solve for $t \in [t_0, t_0 + \Delta t]$

$$\begin{cases} \partial_t n = 0, \\ \partial_t (nu) = 0, \\ \partial_t (nE) = -\sigma_a(\theta^4 - \rho), \\ \eta \partial_t \rho = -\dfrac{1}{\sigma_s} \mathscr{F}^{-1}\Big(\dfrac{P_\varepsilon(\xi)}{Q_\varepsilon(\xi)} \mathscr{F}\rho\Big) + \sigma_a(\theta^4 - \rho), \end{cases}$$

with $n(t_0) = \bar{n}(t_0 + \Delta t)$, $u(t_0) = \bar{u}(t_0 + \Delta t)$, $E(t_0) = \bar{E}(t_0 + \Delta t)$
and $\rho(t_0) = \bar{\rho}(t_0 + \Delta t)$.
$P_\varepsilon / Q_\varepsilon$ is the Pade approximation of Ψ_ε given by
$P_\varepsilon(\xi) = \xi^2/3$ and $Q_\varepsilon(\xi) = 1 + \varepsilon^2 \xi^2/3$.

Table 1: Algorithm for solving the system (5.10).

Step 1 is treated using a classical Lagrange-Projection method. We rewrite the system to be solved in Step 2 as follows

$$\begin{cases} \partial_t n = 0, \\ \partial_t (nu) = 0, \\ \partial_t (nE) = -\sigma_a(\theta^4 - \rho), \\ \eta\Big(\mathrm{I} - \dfrac{\varepsilon^2}{3}\partial_{xx}^2\Big)\partial_t \rho = \dfrac{1}{3\sigma_s}\partial_{xx}^2 \rho + \sigma_a\Big(\mathrm{I} - \dfrac{\varepsilon^2}{3}\partial_{xx}^2\Big)(\theta^4 - \rho). \end{cases} \tag{5.11}$$

Since n and nu remain constant during Step 2, the third equation in (5.11) can be recast as $\frac{R}{\gamma-1} n \partial_t \theta = -\sigma_a(\theta^4 - \rho)$; therefore we actually have to deal with the following system, having unknowns (θ, ρ),

$$\begin{cases} \dfrac{R}{\gamma-1} n\, \partial_t \theta = -\sigma_a(\theta^4 - \rho), \\ \eta\Big(\mathrm{I} - \dfrac{\varepsilon^2}{3}\partial_{xx}^2\Big)\partial_t \rho = \dfrac{1}{3\sigma_s}\partial_{xx}^2 \rho + \sigma_a\Big(\mathrm{I} - \dfrac{\varepsilon^2}{3}\partial_{xx}^2\Big)(\theta^4 - \rho). \end{cases} \tag{5.12}$$

Summing these two equations and integrating with respect to space, we verify the energy conservation

$$\int \Big(\frac{R}{\gamma-1} n\theta + \eta\rho\Big)\,\mathrm{d}x = C^{\mathrm{st}}.$$

Since (5.12) is nonlinear and the space-discretized problem could be stiff, we decide to use an implicit Euler scheme. Let us define the following matrices

$$A = \begin{pmatrix} \mathscr{R} & 0 \\ 0 & \eta(\mathrm{Id} - \varepsilon^2 \frac{\Delta_d}{3}) \end{pmatrix} \quad \text{and} \quad B = \begin{pmatrix} -\sigma_a & \sigma_a \\ \sigma_a(\mathrm{Id} - \varepsilon^2 \frac{\Delta_d}{3\sigma_s}) & \frac{\Delta_d}{3\sigma_s} - \sigma_a(\mathrm{Id} - \varepsilon^2 \frac{\Delta_d}{3}), \end{pmatrix}$$

where Δ_d stands for a discrete Laplacian and $\mathscr{R} = Rn/(\gamma-1)$. The implicit Euler approximation of (5.12) is

$$\begin{pmatrix} \theta^{k+1} \\ \rho^{k+1} \end{pmatrix} = \begin{pmatrix} \theta^k \\ \rho^k \end{pmatrix} + \Delta t A^{-1} B \begin{pmatrix} (\theta^{k+1})^4 \\ \rho^{k+1} \end{pmatrix} = F(\theta^{k+1}, \rho^{k+1}). \tag{5.13}$$

We solve this nonlinear problem by Newton iterations. Let us define $G = I - F$, which is an application of $\mathbb{R}^{2N}$ in $\mathbb{R}^{2N}$. The point $(\theta^{k+1}, \rho^{k+1})$ is therefore a zero of G. In order to solve $G(X) = 0$, the Newton scheme is $X_{s+1} = X_s - [J_G(X_s)]^{-1} G(X_s)$, where J_G denotes the jacobian matrix of G. We have $J_G = I - J_F$ with

$$J_F = \Delta t A^{-1} B \begin{pmatrix} 4\theta^3 & 0 \\ 0 & 1 \end{pmatrix}.$$

The Newton algorithm then reads

$$(A - \Delta t B D_s) W_{s+1} = (A - \Delta t B D_s) W_s - A(W_s - W_0) + \Delta t B \phi(W_s), \tag{5.14}$$

where

$$W_0=(\theta^k,\rho^k)\in\mathbb{R}^{2N},\qquad D_s=\begin{pmatrix}4\theta_s^3 & 0\\ 0 & 1\end{pmatrix},\qquad \varphi(W_s)=(\theta_s^4,\rho_s).$$

We iterate the previous recurrence relation until the relative difference $\|W_{s+1}-W_s\|/\|W_0\|$ becomes smaller than a given tolerance threshold. The Newton scheme (5.14) has some remarkable properties which deserve some comments

- Energy is conserved at each step of the Newton algorithm: a direct computation shows that for any s

$$\sum_j\left(\mathscr{R}\theta_{s,j}+\eta\rho_{s,j}\right)=\sum_j\left(\mathscr{R}\theta_j^k+\eta\rho_j^k\right),$$

  the sum being taken over all indices of the space discretization.

- As ε and/or η go to 0, the scheme is consistent with an implicit Euler time discretization of the corresponding continuous equation.

- The scheme adapts easily to cases where the opacities σ_a depend on the material temperature θ.

Remark 5.1. Since the conservation of energy is a fundamental property of the model, it is important that the numerical method preserves it. Note that a comparable semi-implicit method has been proposed in [28] for a slightly different radiative hydrodynamic model and incorporated in the code Heracles of the French Atomic Energy Commission.

In order to validate the previous algorithm for long times simulation and stability with respect to $\varepsilon,\eta\to 0$, we realize a first simulation issued from [16]: the goal is to recover numerically a shock profile connecting two end states (n_l,u_l,p_l) and (n_r,u_r,p_r). Indeed, a relevant question for applications consists in understanding how the coupling with radiation influences the usual shock structure of the Euler system. We refer to the seminal treatises [44, 58] and to [30] for discussion on physical grounds on this problem. More recently the question has been revisited in [41]. A rigorous analysis of these intricate phenomena is particularly tough. In [37], it has been proved that for shocks having a small enough amplitude, there exists a smooth profile, solution of (5.5) coupled to (5.7) and the stability of these profiles is investigated in [38], in the spirit of [31]. However the problem remains essentially open for large amplitude shocks, and referring to the physical intuition detailed in [41, 44, 58], one can expect the formation of pathological structures, with in particular non monotone temperature profiles (the Zeldovich spikes). Capturing such structure, which can be highly localized, is challenging for numerics and requires carefully developped schemes, even for simplified coupled models see e. g. [2,7, 11,28,49]. For refer to [16] and the references therein for details and recent developments.

According to [16], we set $R=1$, $\gamma=1.4$ $\sigma_a=\sigma_s=1$; the left/right states are given by $n_l=1$, $n_r=3$, $u_l=3$, $u_r=1$, $p_l=1.28$ and $p_r=7.28$. The speed of the shock is given by the standard

Rankine-Hugoniot conditions for the Euler equation and we consider a stationary shock so that the profile stays in the computation domain. For every numerical experiments below, the domain length is set to 80 and is meshed with 1000 points. The time step is computed such that it verifies the CFL condition. The temperature and radiation are fixed to their values at initial time on the boundaries (which also set the value of the pressure). The boundary conditions for the other fluid quantities are transparent (one fixes the values at the boundary to be the adjacent ones in the domain in order to avoid Riemann problem). Figure 10 shows the result obtained with $\varepsilon = 0 = \eta$, as in [16]: since the profile corresponds to the large time asymptotics of the numerical solution there is indeed no significant difference with the solutions computed with different values of the parameters, in agreement with the remark made in Section 4.4. The remarkable point is the non monotone profile of the temperature with a noticeable peak at the front shock.

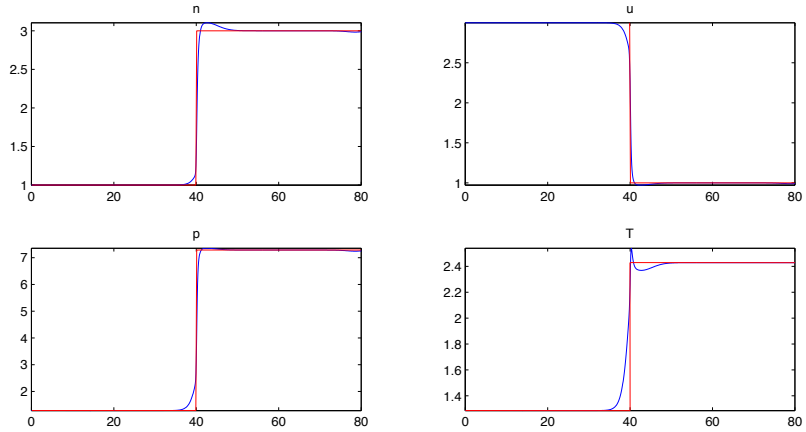

Figure 10: Radiative shock profile: fluid density n, fluid velocity u, pressure p, material temperature T.

For the next test, we start from a constant state for the fluid, initially at rest: $n = 1$, $p = 1$, $u = 0$. We put a hot source of radiation:

$$\rho_{\text{Init}}(x) = 8.10^6 \, \mathbf{1}_{(35,45)}(x) + 1.6.10^8 \, \mathbf{1}_{(30,35)\cup(45,50)}(x),$$

(bearing in mind that the temperature of the radiative field is $\rho^{1/4}$). We display the time evolution in Fig. 11 to 16 for several values of ε and η (while $\sigma_a = \sigma_s = 1$ in all these simulations). This produces quite violent patterns for the fluid density and velocity, as well as it increases the material temperature in the central domain. The shape of the solution is then smoothed as time grows. Compared to the diffusion limit the nonlocal model modifies slightly the details of the solution, especially for short times, where in particular the L^∞ norm of the fluid density can differ noticeably and the temperature spreads more in the domain as ε vanishes.

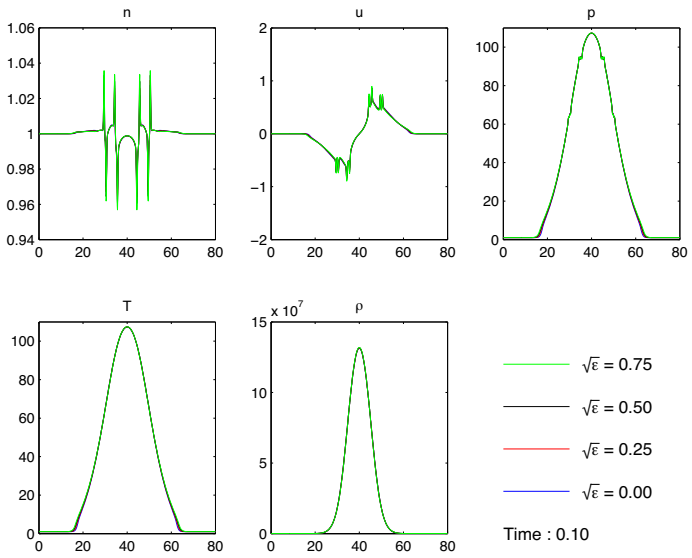

Figure 11: Evolution starting with a constant state and a hot source: $\eta = 0$, $t = 0.1$

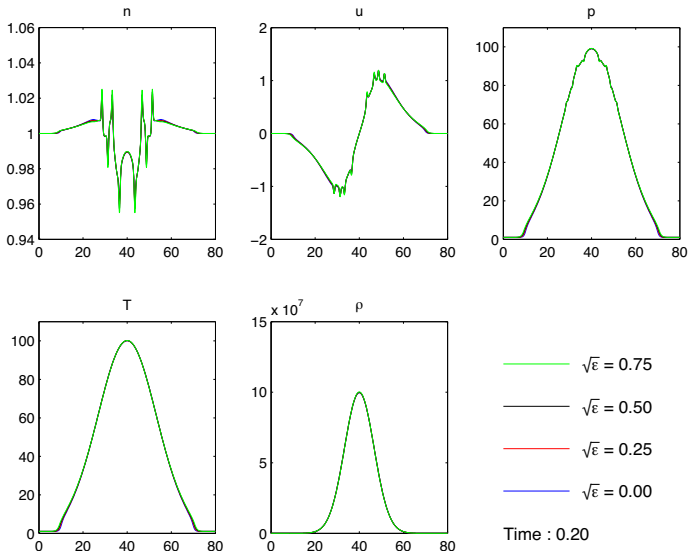

Figure 12: Evolution starting with a constant state and a hot source: $\eta = 0$, $t = 0.2$

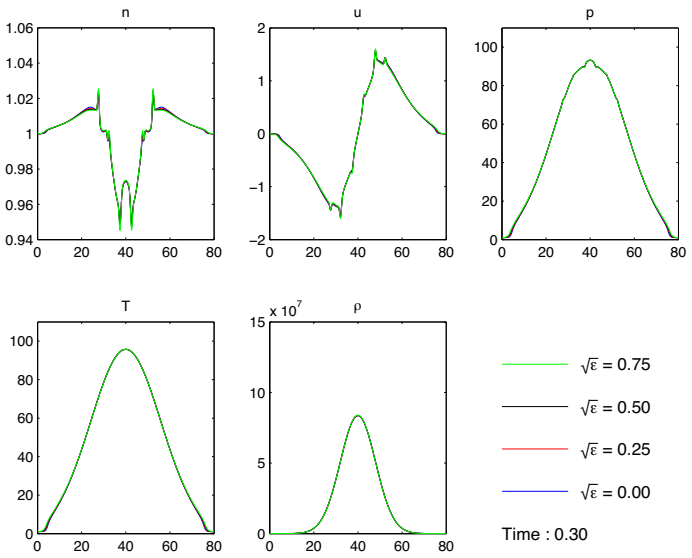

Figure 13: Evolution starting with a constant state and a hot source: $\eta = 0$, $t = 0.3$

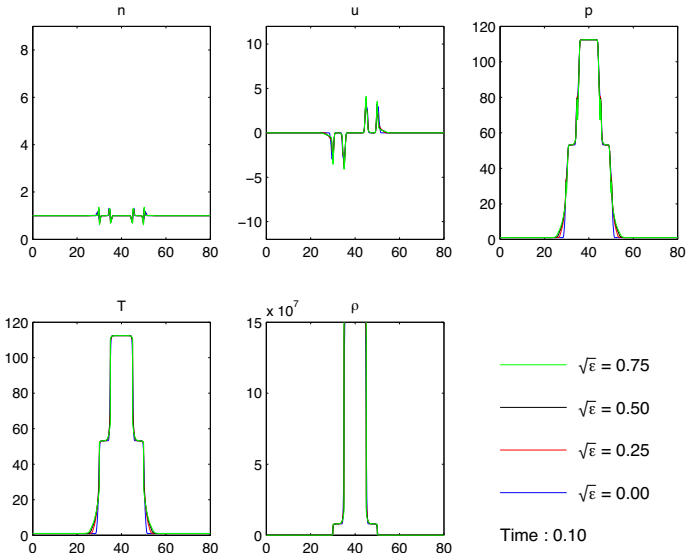

Figure 14: Evolution starting with a constant state and a hot source: $\eta = 1$, $t = 0.1$

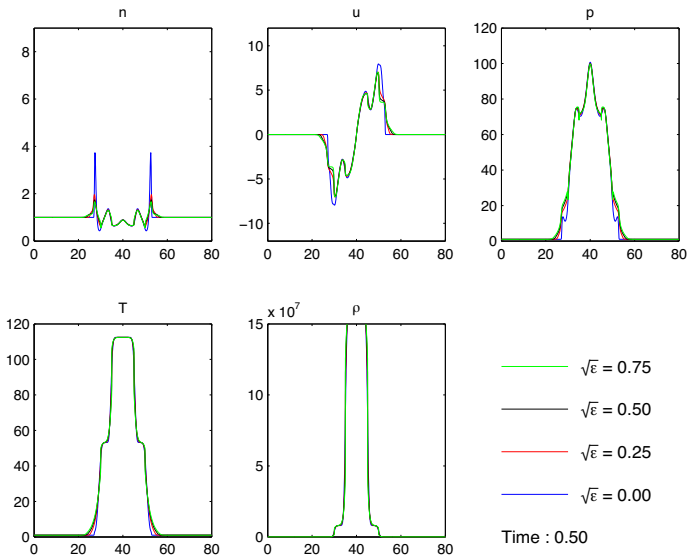

Figure 15: Evolution starting with a constant state and a hot source: $\eta = 1$, $t = 0.5$

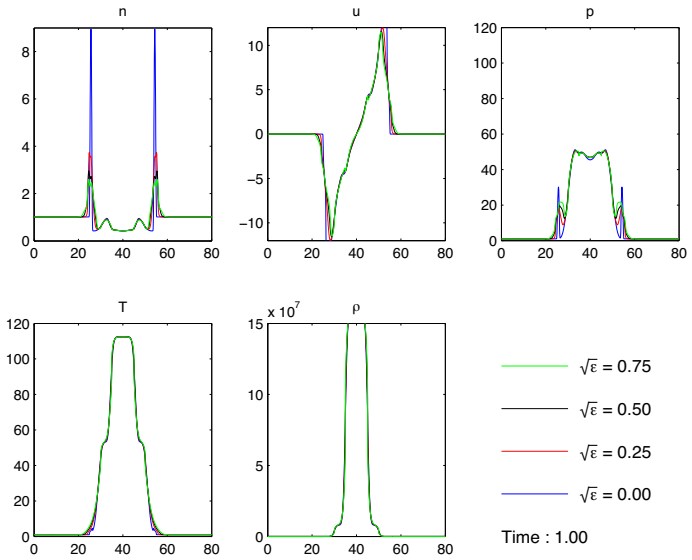

Figure 16: Evolution starting with a constant state and a hot source: $\eta = 1$, $t = 1.0$

Finally, we perform the standard Su-Olson test. It consists of the following very simple coupling between radiation and temperature

$$\begin{cases} \partial_t + \dfrac{v}{\varepsilon}\partial_x f = \dfrac{1}{\varepsilon^2}(\rho - f) + \theta - \rho + S, \\ \partial_t \theta = \rho - \theta \end{cases}$$

with $\rho(t,x)=\int f(t,x,v)\,\mathrm{d}v$ and with the source term

$$S(t,x)=\mathbf{1}_{[0,1]}.$$

The problem is set on $t\geq 0$, $x\in(0,10)$, $v\in(-1,+1)$. It is completed with the initial condition

$$f(t=0,x,v)=10^{-10},\qquad \theta(t=0,x)=10^{-10}.$$

Boundary conditions are also given by this equilibrium state. Proposed in [46, 55] this problem has become a benchmark for radiative transfer codes and models. We refer for instance to [8, 10, 13] in particular for such validation of the $M1$ model. We compare the computations made with the asymptotic preserving scheme introduced in [13] with simulations using the macroscopic model

$$\begin{cases} \partial_t\rho=-\mathscr{F}^{-1}\Big(\Psi_\varepsilon(\xi)\ \mathscr{F}\rho\Big)+\sigma_a(\theta-\rho)+S,\\ \partial_t\theta=\sigma_a(\rho-\theta). \end{cases}$$

Actually, since we are not in the periodic case, we cannot use easily this pseudo-differential equation; instead, we use the simple approximation

$$\partial_t\rho=-\mathscr{F}^{-1}\Big(\frac{\xi^2/3}{1+\varepsilon^2\xi^2/3}\mathscr{F}\rho\Big)+\sigma_a(\theta-\rho)+S,$$

which is amenable to the numerical treatment detailed above. In Fig. 17 we plot the density in log scales. The results are quite surprising and difficult to interpret. Qualitatively we find the expected shape, but the values are not satisfactory. In particular, surprisingly, the slope increases as ε goes to 0, conversely to the expected behavior. We do not have explanation of this deceptive behavior, except the fact that the source term is highly singular and maybe not well adapted when applying the Laplace operator.

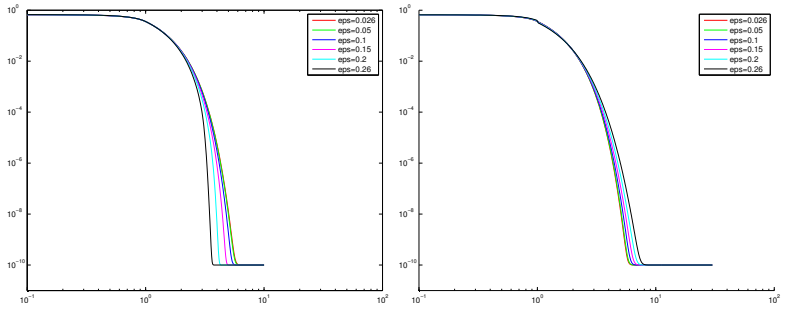

(a) AP scheme (b) Reduced model

Figure 17: Su-Olson test: Comparison of the density at time final $T=1$ in log scales with an AP kinetic scheme and the reduced model for several values of ε.

6 Conclusions

By revisiting an approach used in plasma physics, we present a possible derivation of a non local model, alternative to moment system closure approximation of kinetic equations. We investigate a few properties of the nonlocal model, which is of pseudo-differential nature. In particular, we show the consistency with the diffusion asymptotics. We discuss several approximations of the underlying pseudo-differential operator and we design numerical schemes for evaluating the solution. The simulation reveal, as for the plasma physics model [24], that such nonlocal model should be used with care. On the one hand, it offers a cheap evaluation of macroscopic quantities, preserving steep gradients better than the diffusion limit, and it can be easily incorporated in coupled systems describing complex physics. On the other hand, its range of validity and the accuracy of the fitting with the kinetic model have limitations. This work is a first attempt that focuses on very simple models and we expect it might help in understanding the limitation of this approach, in deriving suitable cure as well as designing well-suited numerical schemes.

Acknowledgments

We thank J.-F. Clouet who introduced the problem to us and pointed out many references on nonlocal temperature models.

References

[1] F. Alouani Bibi and J.-P. Matte. Nonlocal electron heat transport and electron-ion energy transfer in the presence of strong collisional heating. *Laser and Particle Beams*, 22:103–108, 2004.

[2] E. Audit, P. Charrier, J.-P. Chièze, and B. Dubroca. A radiation-hydrodynamics scheme valid from the transport to the diffusion limit. *Preprint* `arXiv:astro-ph/0206281`, 2002.

[3] C. Bardos, F. Golse, and B. Perthame. The Rosseland approximation for the radiative transfer equations. *Comm. Pure Appl. Math.*, 40(6):691–721, 1987.

[4] C. Bardos, F. Golse, and B. Perthame. Erratum to the article: "The Rosseland approximation for the radiative transfer equations". *Comm. Pure Appl. Math.*, 42(6):891–894, 1989.

[5] C. Bardos, F. Golse, B. Perthame, and R. Sentis. The nonaccretive radiative transfer equations: existence of solutions and Rosseland approximation. *J. Funct. Anal.*, 77(2):434–460, 1988.

[6] C. Bardos, R. Santos, and R. Sentis. Diffusion approximation and computation of the critical size. *Trans. Amer. Math. Soc.*, 284(2):617–649, 1984.

[7] C. Berthon, P. Charrier, and B. Dubroca. An HLLC scheme to solve the $M1$ model of radiative transfer in two space dimensions. *J. Sci. Comput.*, 31(3):347–389, 2007.

[8] C. Berthon, J. Dubois, and R. Turpault. Numerical approximation of the $M1$-model. In *Mathematical Models and Numerical Methods for Radiative Transfer (T. Goudon Ed.)*, volume 28 of *Panoramas et Synthèses, SMF*, to appear.

[9] C. Buet and S. Cordier. Asymptotic preserving scheme and numerical methods for radiative hydrodynamic models. *C. R. Math. Acad. Sci. Paris*, 338(12):951–956, 2004.
[10] C. Buet and B. Després. Asymptotic preserving and positive schemes for radiation hydrodynamics. *J. Comput. Phys.*, 215(2):717–740, 2006.
[11] B. Buffa and B. Dubroca. *Lectures Notes MathMeca*. Université Bordeaux 1, 1999.
[12] J. A. Carrillo, I. M. Gamba, A. Majorana, and C.-W. Shu. A WENO-solver for the transients of BoltzmannPoisson system for semiconductor devices: performance and comparisons with Monte-Carlo methods. *J. Comput. Phys.*, 184:498–525, 2003.
[13] J.-A. Carrillo, Th. Goudon, P. Lafitte, and F. Vecil. Kinetic equations, diffusion asymptotics and moment closures. *J. Sci. Comput.*, 36(1):113–149, 2008.
[14] J. A. Carrillo and F. Vecil. Nonoscillatory interpolation methods applied to Vlasov-based models. *SIAM J. Sci. Comput.*, 29(3):1179–1206 (electronic), 2007.
[15] J.-F. Coulombel, F. Golse, and T. Goudon. Diffusion approximation and entropy-based moment closure for kinetic equations. *Asymptot. Anal.*, 45(1-2):1–39, 2005.
[16] J.-F. Coulombel and P. Lafitte. Computation of shock profiles in radiative hydrodynamics. *Comm. Comput. Physics*, 6(5):1118–1136, 2009.
[17] R. Dautray and J.-L. Lions. *Analyse mathématique et calcul numérique pour les sciences et les techniques*. Masson, 1985.
[18] P. Degond, T. Goudon, and F. Poupaud. Diffusion limit for nonhomogeneous and non-micro-reversible processes. *Indiana Univ. Math. J.*, 49(3):1175–1198, 2000.
[19] L. Desvillettes and F. Golse. A remark concerning the Chapman-Enskog asymptotics. In *Advances in Kinetic Theory and Computing*, volume 22 of *Series on Advances in Mathematics for Applied Sciences*, pages 191–203. World Scientific Publications, 1994.
[20] B. Dubroca. *Etude de régimes microscopiques, macroscopiques et transitionnels basés sur des équations cinétiques : modélisation et approximation numérique*. Habilitation à diriger les recherches. Université Bordeaux 1, 2000.
[21] B. Dubroca and J.-L. Feugeas. Etude théorique et numérique d'une hiérarchie de modèles aux moments pour le transfert radiatif. *C. R. Acad. Sci. Paris Sér. I Math.*, 329(10):915–920, 1999.
[22] B. Engquist and A. Majda. Absorbing boundary conditions for the numerical simulation of waves. *Math. Comp.*, 31(139):629–651, 1977.
[23] B. Engquist and A. Majda. Radiation boundary conditions for acoustic and elastic wave calculations. *Comm. Pure Appl. Math.*, 32(3):314–358, 1979.
[24] E. M. Epperlein and R. W. Short. A practical nonlocal model for electron heat transport in laser plasmas. *Phys. Fluids B*, 3(11):3092–3098, 1991.
[25] J.-L. Feugeas. A hierarchy of nonlocal models for the radiative transfer equation. *Laser and Particle Beams*, 22:121–127, 2004.
[26] J. Fort. Information theoretical approach to radiative transfer. *Physica A*, 243:275–303, 1997.
[27] P. Godillon-Lafitte and Th. Goudon. A coupled model for radiative transfer: Doppler effects, equilibrium and non equilibrium diffusion asympotics. *SIAM MMS*, 4:1245–1279, 2005.
[28] M. Gonzalez. *Contribution à l'étude numérique de l'hydrodynamique radiative : des expériences de chocs radiatifs aux jets astrophysiques*. PhD thesis, Univ. Paris-Sud XI, 2006.
[29] T. Goudon and F. Poupaud. Approximation by homogenization and diffusion of kinetic equations. *Comm. Partial Differential Equations*, 26(3-4):537–569, 2001.
[30] B. S. Heaslet and M. A. Baldwin. Predictions of the structure of radiation-resisted shock waves. *Phys. Fluids*, 6:781–791, 1963.
[31] S. Kawashima, Y. Nikkuni, and S. Nishibata. The initial value problem for hyperbolic-elliptic

coupled systems and applications to radiation hydrodynamics. In *Analysis of systems of conservation laws (Aachen, 1997)*, volume 99 of *Chapman & Hall/CRC Monogr. Surv. Pure Appl. Math.*, pages 87–127. Chapman & Hall/CRC, Boca Raton, FL, 1999.

[32] C. D. Levermore. A Chapman–Enskog approach to flux limited diffusion theory. *Technical Report, Lawrence Livermore Laboratory*, UCID-18229, 1979.

[33] C. D. Levermore. Moment closure hierarchies for kinetic theories. *J. Statist. Phys.*, 83(5-6):1021–1065, 1996.

[34] C. D. Levermore. Entropy-based moment closures for kinetic equations. In *Proceedings of the International Conference on Latest Developments and Fundamental Advances in Radiative Transfer (Los Angeles, CA, 1996)*, volume 26, pages 591–606, 1997.

[35] C. D. Levermore and W. J. Morokoff. The Gaussian moment closure for gas dynamics. *SIAM J. Appl. Math.*, 59(1):72–96 (electronic), 1999.

[36] C. D. Levermore and G. C. Pomraning. A flux-limited diffusion theory. *The Astrophys. J*, 248:321–334, 1981.

[37] C. Lin, J.-F. Coulombel, and Th. Goudon. Shock profiles for non equilibrium radiating gases. *Physica D*, 218(1):83–94, 2006.

[38] C. Lin, J.-F. Coulombel, and Th. Goudon. Asymptotic stability of shock profiles in radiative hydrodynamics. *C. R. Acad. Sci. Paris Sér. I Math.*, 345(11):625–628, 2007.

[39] P.-L. Lions and G. Toscani. Diffuse limit for finite velocity boltzmann kinetic models. *Rev. Mat. Ib.*, 13:473–513, 1997.

[40] R. B. Lowrie, J. E. Morel, and J. A. Hittinger. The coupling of radiation and hydrodynamics. *The Astrophys. J.*, 521:432–450, 1999.

[41] R. B. Lowrie and R. M. Rauenzahn. Shock wave solutions for equilibrium-diffusion radiation hydrodynamics. *Shock Waves*, 16(6):445–453, 2007. (Los Alamos Technical Report LA-UR-06-8283).

[42] J.-F. Luciani and P. Mora. Nonlocal electron transport in laser created plasmas. *Laser and Particles Beams*, 12(3):387–400, 1994.

[43] J.-F. Luciani, P. Mora, and J. Virmont. Nonlocal heat transport due to steep temperature gradient. *Physical Rev. Lett.*, 51(18):1664–1667, 1983.

[44] B. Mihalas and D. Weibel-Mihalas. *Foundations of radiation hydrodynamics*. Oxford University Press, 1984.

[45] Ph. Nicolaï, J.-L. Feugeas, and G. Schurtz. A practical nonlocal model for heat transport in magnetized plasmas. *Physics of Plasmas*, 13:032701–1–032701–13, 2006.

[46] G. Olson, L. Auer, and M. Hall. Diffusion, P1, and other approximate forms of radiation transport. *J. Quant. Spectrosc. Radiat. Transf.*, 64:619–634, 2000.

[47] M. Parisot. *Analysis and simulation of non-local models in plasma physics*. PhD thesis, Univ. des Sciences et Technonologies de Lille. In preparation.

[48] P. Reuss. *Neutron physics*. EDP Sciences, 2008.

[49] J.-F. Ripoll, B. Dubroca, and E. Audit. A factored operator method for solving coupled radiation-hydrodynamics models. *Transp. Theory Stat. Physics*, 31(4-6):531–558, 2002.

[50] G. Schurtz, S. Gary, C. Chenais-Popovic, J.-C. Gauthier, F. Thais, J. Breil, Durut F., Feugeas J.-L., P.-H. Maire, P. Nicolaï, O. Peyrusse, C. Reverdin, G. Soullié, V. Tikhonchuk, B. Villette, and C. Fourment. Revisiting nonlocal electron-energy transport in inertial-fusion conditions. *Phys. Rev. Lett.*, 98:095002–1–095002–4, 2007.

[51] G. Schurtz, Ph. Nicolaï, and M. Busquet. A nonlocal electron conduction model for multidimensional radiation hydrodynamics codes. *Physics of Plasmas*, 7(10):4238–4249, 2000.

[52] M. Seaïd, A. Klar, and B. Dubroca. Flux limiters in the coupling of radiation and hydrody-

namic models. *J. Comput. Appl. Math.*, 168(1-2):425–435, 2004.

[53] M. Shäfer, M. Frank, and C. D. Levermore. Diffusive corrections to P_N approximations. *Preprint*, 2009.

[54] A. W. Smith and K. F. Brennan. Comparison of non-parabolic hydrodynamic simulations for semiconductor devices. *Solid-state Electronics*, 39(7):1055–1063, 1996.

[55] B. Su and G. Olson. Benchmark results for the non-equilibrium Marshak diffusion problem. *J. Quant. Spectrosc. Radiat. Transf.*, 56(3):337–351, 1996.

[56] I. Teleaga, M. Seaïd, I. Gasser, A. Klar, and J. Struckmeier. Radiation models for thermal flows at low Mach number. *J. Comput. Phys.*, 215(2):506–525, 2006.

[57] S. Weber, G. Riazuelo, P. Michel, R. Loubère, F. Walraet, V. Tikhonchuk, V. Malka, J. Ovadia, and G. Bonnaud. Modeling of laser-plasma interaction on hydrodynamic scales: Physics development and comparison with experiments. *Laser and Particles Beams*, 22:189–195, 2004.

[58] Ya. B. Zeldovich, Yu. P. Raizer. *Physics of shock waves and high-temperature hydrodynamic phenomena*. Academic Press, 1966.